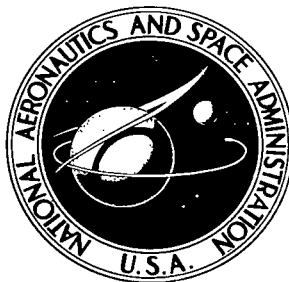


NASA TECHNICAL NOTE



NASA TN D-4679

001

NASA TN D-4679

LOAN COPY: R
AFWL (W
KIRTLAND AFI



CALIBRATION OF 30° INCLUDED-ANGLE CONE
FOR DETERMINING LOCAL FLOW CONDITIONS
IN MACH NUMBER RANGE OF 1.51 TO 3.51

by Walter A. Vahl and Robert L. Weirich

Langley Research Center

Langley Station, Hampton, Va.



CALIBRATION OF 30° INCLUDED-ANGLE CONE FOR DETERMINING
LOCAL FLOW CONDITIONS IN MACH NUMBER RANGE
OF 1.51 TO 3.51

By Walter A. Vahl and Robert L. Weirich

Langley Research Center
Langley Station, Hampton, Va.

NATIONAL AERONAUTICS AND SPACE ADMINISTRATION

For sale by the Clearinghouse for Federal Scientific and Technical Information
Springfield, Virginia 22151 - CFSTI price \$3.00

CALIBRATION OF 30° INCLUDED-ANGLE CONE FOR DETERMINING
LOCAL FLOW CONDITIONS IN MACH NUMBER RANGE
OF 1.51 TO 3.51

By Walter A. Vahl and Robert L. Weirich
Langley Research Center

SUMMARY

A 30° included-angle cone was calibrated to permit determination of the local Mach number, total pressure, and flow angles from measurements of total pressure at the cone apex and static pressure at four equally spaced orifices on the cone surface. The calibration data were obtained at Mach numbers of 1.51, 2.37, 2.96, and 3.51 over an angle-of-pitch range of 0° to 20°. The test Reynolds number ranged from 6.56×10^6 to 9.85×10^6 per meter. The test results indicate that the accuracy of Mach number determination varies from approximately ± 0.010 to ± 0.050 at Mach numbers of 1.51 to 3.51, respectively. The accuracy of the total-pressure measurement varies from approximately ± 0.5 percent to ± 4.5 percent at Mach numbers of 1.51 to 3.51, respectively. The flow angles may be determined within approximately $\pm 0.25^\circ$ for angles less than 10° and within approximately $\pm 0.50^\circ$ for angles greater than 10° . Generally, an iterative procedure is required only for accurate determination of the Mach number and total pressure at Mach numbers near or greater than 2.37, with angles of pitch above approximately 10° .

INTRODUCTION

In order to facilitate a survey of the flow field around a supersonic transport model, a rake of 30° included-angle cones was calibrated for determining local values of Mach number, total pressure, and flow angles. Representative results of a typical cone of the rake are presented herein.

A similar calibration of a 40° included-angle cone is given in reference 1. This calibration covered a Mach number range of 1.72 to 2.46. The present calibration covers a broader range of Mach number of 1.51 to 3.51. The data presented in this paper follow the format of reference 1.

SYMBOLS

C_p	pressure coefficient, $\frac{p_s - p_1}{q_1}$
M_1	Mach number ahead of normal shock wave at cone apex
$\left(\frac{\Delta p}{q_1}\right)_\epsilon$	difference in pressure coefficient between orifices c and a, $\frac{p_{s_c} - p_{s_a}}{q_1}$ (fig. 2)
$\left(\frac{\Delta p}{q_1}\right)_\sigma$	difference in pressure coefficient between orifices d and b, $\frac{p_{s_d} - p_{s_b}}{q_1}$ (fig. 2)
p_{t_2}	pitot pressure behind normal shock wave at cone apex, newtons/meter ²
p_{t_1}	total pressure ahead of normal shock wave at cone apex, newtons/meter ²
p_s	static pressure on cone surface, newtons/meter ²
p_1	static pressure ahead of normal shock wave at cone apex, newtons/meter ²
\bar{p}	arithmetic mean of four static pressures, $\frac{1}{4}(p_{s_a} + p_{s_b} + p_{s_c} + p_{s_d})$, newtons/meter ²
q_1	dynamic pressure ahead of normal shock wave at cone apex, newtons/meter ²
u_1, v_1, w_1	velocities in X, Y, and Z directions, meters/second (fig. 2)
V_1	velocity ahead of normal shock wave at cone apex, meters/second
X, Y, Z	body axes (fig. 2)
α	angle of attack, degrees (fig. 2)
β	angle of sideslip, degrees (fig. 2)
ϵ	angle of downwash, degrees (fig. 2)
θ	angle of pitch (between cone axis and velocity vector), degrees (fig. 2)

σ angle of sidewash, degrees (fig. 2)
 ϕ radial or roll angle, degrees (fig. 2)

Subscripts:

1 conditions ahead of normal shock wave at cone apex
2 conditions behind normal shock wave at cone apex
a,b,c,d positions of orifices on cone surface (fig. 2)
 θ value at angle of pitch
 $\theta = 0$ value at zero angle of pitch

APPARATUS

Model

The model consisted of a rake containing four cones, each having an included angle of 30° and a maximum diameter of 0.635 cm. Each cone contained a sharp-lipped total-pressure orifice at the apex and four equally spaced static-pressure orifices located at the same longitudinal cone station. All orifice diameters were 0.0508 cm. Angular and linear placement of the static orifices was within $\pm 3.0^\circ$ and ± 0.0178 cm, respectively, of the desired locations. Details of the calibration rake and orifice locations are shown in figures 1 and 2.

In general, the selection of the cone angle was based on the following considerations:

(1) A small cone angle permits a lower minimum Mach number before shock detachment occurs with resulting regions of subsonic flow over the cone surface.

(2) A large cone angle affords an increased pressure differential between opposite orifices when the cone is inclined and hence permits greater sensitivity in determining flow angles.

(3) A large cone angle is advantageous in delaying the onset of flow separation over the cone surface to large flow angles.

(4) A small cone angle tends to allow a closer spacing of the cones without mutual interference. In particular, where multiple cones are used, as in a flow-survey rake, a closer spacing of the flow-field data points may be obtained.

Because the rake of cones was intended for a survey of the flow field of a supersonic transport model, a compromise of the preceding considerations, along with consideration of the expected ranges of the variables to be determined, led to the selection of the 30° cone angle.

Tunnel

The investigation was conducted in both the high Mach number and low Mach number test sections of the Langley Unitary Plan wind tunnel. Each test section is approximately 1.22 meters square and 2.13 meters long. The tunnel is a variable-pressure, continuous-flow facility with asymmetric sliding-block nozzles which permit continuous variation of the free-stream Mach number. The Mach number range of the high Mach number test section is 2.29 to 4.65, and the range of the low Mach number test section, 1.50 to 2.90.

TEST CONDITIONS AND PROCEDURE

The calibration data were obtained at Mach numbers of 1.51, 2.37, 2.96, and 3.51. In addition, a few selected data points were recorded at Mach numbers of 1.85, 2.01, 2.62, and 3.25. The stagnation temperature was 338.7° K for all Mach numbers. The test Reynolds number ranged from 6.56×10^6 to 9.85×10^6 per meter. The dewpoint, measured at stagnation pressure, was maintained below 238.7° K to minimize condensation effects.

The tests were conducted through an angle-of-pitch range of 0° to 20°. Data were recorded at regular increments in roll angle. Because of mechanical limitations of the support apparatus, the calibration was performed only through the range of positive pitch angles. Before data were recorded at angles of pitch, the model support mechanism was positioned so that the rake was in approximately the same area of the test section as that which it occupied at zero angle of pitch. In this manner, effects of possible deviation in flow angularity throughout the test section were minimized. In addition, the axis of rotation of the rake was coincident with the center line of one of the cones. At each angle of pitch, the rake of four cones was rotated through a roll-angle range of $\pm 90^\circ$, thereby providing data corresponding to upright and inverted cone positions for each pair of diametrically opposed orifices.

A comparison of the data was made for the four cones at each Mach number with the pair of diametrically opposed orifices located in the pitch plane in both the upright and inverted positions ($\phi = -90^\circ$ and 90°). For each cone, the slopes of the curves of $(\Delta p/q_1)_\epsilon$ as a function of pitch angle were the same for both the upright and inverted

positions, which indicates that the effect on the data of variations in the dimensions of the cones and in the angular and linear spacing of the orifices within the specified tolerances was negligible.

Based on repeatability of data and calibration of the instrumentation, the accuracy ranges of the experimentally measured quantities at each test Mach number are as follows:

C_p	± 0.005
\bar{p}/p_{t_2}	± 0.002
M_1	± 0.005
θ , deg	± 0.1
ϕ , deg	± 0.1

RESULTS AND DISCUSSION

Representative results for one of the 30° included-angle cones of the calibration rake are presented in a manner similar to that of reference 1. A description of how each of the local flow parameters may be determined through the use of the included charts is given. In addition, a typical example of the numerical procedure involved is contained in the appendix.

Pressure Distribution

Presented in figure 3 are the pressure distributions on the cone surface for the Mach numbers and angles of pitch of the tests. All regions have positive pressure coefficients, with the exception of a few small regions of negative pressure coefficients on the leeward side of the cone, which occurred when the cone was at angles of pitch of 17.5° and 20°. In figure 4, a few of the measured pressure coefficients are compared with those theoretically determined. The calculated values obtained by using the first-order nonlinear theory of reference 2 are considerably less than the experimental values near the top and bottom of the cone. Fair agreement is obtained along the side of the cone. The second-order nonlinear theory of reference 3 gives good agreement with the experimental results over the complete radial-angle range. Use of reference 4 was made to obtain constants required in the application of references 2 and 3. Similar agreement between experimental and theoretical data is reported in reference 1.

Mach Number

The local Mach number may be determined for zero angle of pitch from the ratio of the average static pressure on the cone surface to the pitot pressure. Values of this ratio

obtained from measured pressures are shown in figure 5 along with those theoretically determined by using reference 5. The values of Mach number used in preparation of this figure were determined from the ratio of the measured values of the pitot pressure to the test-section stagnation pressure by use of the normal-shock-wave relations. As can be seen, agreement is quite good over most of the Mach number range.

For cases of flow inclination to the cone axis, the ratio of the average of the four static pressures measured at the cone surface (\bar{p}) to the pitot pressure may be used to determine the Mach number, provided a procedure for correcting the value of this ratio for inclination effects is followed. Figure 6 indicates the experimentally determined effect of pitch on the ratio of the average static pressure to the pitot pressure for each Mach number of the tests. Data for corresponding roll angles were averaged, for example, data measured at $\phi = 10^\circ, -10^\circ, 80^\circ,$ and -80° , since, from symmetry, the averaged values of the static pressures would be expected to be equal. Some of the test data were recorded at roll-angle increments of 15° . In order to present all data at 10° increments, these data were cross-plotted, and the corresponding values for 10° roll-angle increments were determined. These cross-plotted data are indicated by the dashed curves in the figures. As can be seen by comparing figures 6(a) to 6(d), the departure of the pressure ratio from that at zero angle of pitch increases with increasing pitch angle. Further, the parameter plotted changes from values less than 1.0 to values greater than 1.0 as the Mach number increases from 1.51 to 3.51.

The procedure to be followed in determining the local Mach number is first to assume that $\theta = 0^\circ$. Through the use of figure 5, a first approximation to the Mach number may be obtained for the measured ratio of \bar{p}/p_{t2} . In order to correct this Mach number for flow inclination to the cone axis, the values of the local flow angles must first be known. These angles may be determined by following the procedure outlined under the heading "Flow Angles." By knowing the values of the local flow angles, a correction factor for \bar{p}/p_{t2} may then be determined from figure 6 and a new value of \bar{p}/p_{t2} corresponding to $\theta = 0^\circ$ computed. (See example in appendix.) A second approximation to the local Mach number may now be made from figure 5. In general, an iterative procedure is followed until the Mach number approximation is within the desired limits. Usually, for small angles of pitch, the first approximation is sufficient. For Mach numbers near or greater than 2.37, with angles of pitch above approximately 10° , an iterative procedure is required. One iteration normally provides a satisfactory value. A similar iterative procedure was also found adequate in reference 1.

Flow Angles

The flow angles are determined by the differences in pressure on the cone surface between the diametrically opposed static orifices. The measured pressure differences

obtained for each Mach number of the calibration tests are presented in figure 7. As can be seen, the data do not pass through the origin. This is probably due to small effects of misalignment and flow angularity.

The data from figure 7 have been replotted in figure 8 so that values of θ and ϕ may be read directly for measured values of $(\Delta p/q_1)_\epsilon$ and $(\Delta p/q_1)_\sigma$. These data were first shifted so that each curve in figure 7 would pass through the origin. Because of symmetry, values of θ and ϕ for each quadrant may be obtained from the data presented in one quadrant only by using the sign convention indicated in figure 8. A comparison of figures 8(b) and 8(c) for Mach numbers of 2.37 and 2.96, respectively, shows negligible or small effect of Mach number on values of $(\Delta p/q_1)_\epsilon$ and $(\Delta p/q_1)_\sigma$. However, at a Mach number of 1.51 (fig. 8(a)) and for angles of pitch above approximately 8° at a Mach number of 3.51 (fig. 8(d)), there is considerable variation of the values of $(\Delta p/q_1)_\epsilon$ and $(\Delta p/q_1)_\sigma$ from those obtained at Mach numbers of 2.37 and 2.96.

In order to determine the flow angles ϵ and σ in terms of θ and ϕ , the following relations may be used:

$$\tan \epsilon = -\tan \theta \cos \phi$$

$$\tan \sigma = \tan \theta \sin \phi$$

Figure 9 presents values of ϵ and σ for values of $(\Delta p/q_1)_\epsilon$ and $(\Delta p/q_1)_\sigma$ so that these angles may be obtained directly from the measured pressure differences between diametrically opposed static-pressure orifices. The sign convention to be used for each of the quadrants is indicated in figure 9.

In order to determine the angles of attack and sideslip, the following relations may be used:

$$\tan \alpha = \tan \theta \cos \phi$$

$$\sin \beta = -\sin \theta \sin \phi$$

Total Pressure

The local total pressure is determined from the pitot pressure and the normal-shock-wave relations. For the scope of the present tests, figure 10 shows the measured pitot pressure to be unaffected by variation of the angle of pitch at each of the test Mach numbers.

Accuracy of Results

Use of the data and methods in this paper, along with cones of similar tolerances and instrumentation of similar accuracy should permit accuracies in determining the

local flow parameters, based on excursions from the average, as follows:

M ₁	M ₁	P _{t1} , percent	Accuracy	
			ε or σ, deg	
			Range	Accuracy
1.51	±0.010	±0.5	0 to 15	±0.25
2.37	±0.020	±1.5	0 to 10	±0.25
			> 10	±.50
2.96	±0.035	±3.0	0 to 10	±0.25
			> 10	±.50
3.51	±0.050	±4.5	0 to 10	±0.25
			> 10	±.50

It should be recognized, however, that errors larger than these could result from measurements in the immediate vicinity of abrupt flow discontinuities.

SUMMARY OF RESULTS

A 30° included-angle cone has been calibrated at Mach numbers of 1.51, 2.37, 2.96, and 3.51 at angles of pitch from 0° to 20°. Through use of the measured cone pressures and the calibration charts presented, local values of Mach number, total pressure, and flow angles may be determined. The accuracy of Mach number determination varies from approximately ±0.010 to ±0.050 at Mach numbers of 1.51 to 3.51, respectively. The accuracy of the total-pressure measurement varies from approximately ±0.5 percent to ±4.5 percent at Mach numbers of 1.51 to 3.51, respectively. The flow angles may be determined within approximately ±0.25° for angles less than 10° and within approximately ±0.50° for angles greater than 10°. Generally, an iterative procedure is required only for accurate determination of the Mach number and total pressure at Mach number near or greater than 2.37, with angles of pitch above approximately 10°.

Langley Research Center,
National Aeronautics and Space Administration,
Langley Station, Hampton, Va., April 5, 1968,
720-03-01-02-23.

APPENDIX

NUMERICAL EXAMPLE

In order to illustrate the use of the described procedure for determining the local values of the Mach number, total pressure, and flow angles from the measured cone static and total pressures, a numerical example is given. The assumed pressures are

$$p_{s_a} = 5611.6 \text{ N/m}^2$$

$$p_{s_b} = 6444.7 \text{ N/m}^2$$

$$p_{s_c} = 10\,619.9 \text{ N/m}^2$$

$$p_{s_d} = 9015.9 \text{ N/m}^2$$

$$p_{t_2} = 37\,528.6 \text{ N/m}^2$$

The arithmetic mean of the four static pressures is

$$\bar{p} = \frac{1}{4}(p_{s_a} + p_{s_b} + p_{s_c} + p_{s_d}) = 7923.0 \text{ N/m}^2$$

and the ratio of this static pressure to the pitot pressure is $\bar{p}/p_{t_2} = 0.211$. By assuming first that $\theta = 0^\circ$, a tentative Mach number of 2.50 is obtained from figure 5. For $\theta = 0^\circ$, the total-pressure ratio p_{t_2}/p_{t_1} is given by the theoretical normal-shock-wave relations tabulated in reference 6. For $M_1 = 2.50$, this ratio is $p_{t_2}/p_{t_1} = 0.4990$, and the total pressure p_{t_1} is

$$p_{t_1} = \frac{(p_{t_2})_{\theta}}{(p_{t_2}/p_{t_1})_{\theta=0}} = \frac{37\,528.6}{0.4990} = 75\,207.6 \text{ N/m}^2$$

The dynamic pressure q_1 is given by

$$q_1 = \left(\frac{q_1}{p_{t_1}}\right) p_{t_1} = 0.2561(75\,207.6) = 19\,260.7 \text{ N/m}^2$$

where the ratio q_1/p_{t_1} is given by the theoretical isentropic flow relations also tabulated in reference 6. Dividing the pressure differences across both pairs of orifices by the dynamic pressure gives

$$\left(\frac{\Delta p}{q_1}\right)_\epsilon = \frac{p_{s_c} - p_{s_a}}{q_1} = \frac{10\,619.9 - 5611.6}{19\,260.7} = 0.260$$

APPENDIX

$$\left(\frac{\Delta p}{q_1}\right)_\sigma = \frac{p_{sd} - p_{sb}}{q_1} = \frac{9015.9 - 6444.7}{19\,260.7} = 0.133$$

The downwash and sidewash angles from figure 9(b) are $\epsilon = -7.9^\circ$ and $\sigma = 3.8^\circ$. In order to correct the Mach number, the angles of pitch and roll must be known. From figure 8(b), $\theta = 9.0^\circ$ and $\phi = 25.5^\circ$. The correction factor from figure 6(b) is

$$\frac{(\bar{p}/p_{t2})_\theta}{(\bar{p}/p_{t2})_{\theta=0}} = 1.015$$

The corrected value of \bar{p}/p_{t2} corresponding to $\theta = 0^\circ$ is

$$\frac{\bar{p}}{p_{t2}} = \frac{(\bar{p}/p_{t2})_\theta}{(\bar{p}/p_{t2})_\theta / (\bar{p}/p_{t2})_{\theta=0}} = \frac{0.211}{1.015} = 0.208$$

From figure 5, the second approximation to the Mach number is $M_1 = 2.53$. Using this new Mach number gives $p_{t2}/p_{t1} = 0.4871$ from reference 6. Because the angle of pitch has no effect on the pitot pressure for angles less than 20° (fig. 10), the pitot pressure need not be corrected to an equivalent value at $\theta = 0^\circ$. The second approximation to the total pressure is

$$p_{t1} = \frac{(p_{t2})_\theta}{(p_{t2}/p_{t1})_{\theta=0}} = \frac{37\,528.6}{0.4871} = 77\,045.0 \text{ N/m}^2$$

and the dynamic pressure is

$$q_1 = \left(\frac{q_1}{p_{t1}}\right) p_{t1} = (0.2503)(77\,045.0) = 19\,284.4 \text{ N/m}^2$$

Because the second determination of the dynamic pressure is essentially the same as the first, the angles of pitch and roll need no correction. Further iteration is unnecessary because the correction factors of figure 6 would be unchanged.

REFERENCES

1. Centolanzi, Frank J.: Characteristics of a 40° Cone for Measuring Mach Number, Total Pressure, and Flow Angles at Supersonic Speeds. NACA TN 3967, 1957.
2. Staff of Comput. Section, Center of Anal. (Under dir. of Zdeněk Kopal): Tables of Supersonic Flow Around Yawing Cones. Tech. Rep. No. 3 (NOrd Contract No. 9169), Massachusetts Inst. Technol., 1947.
3. Staff of Comput. Section, Center of Anal. (Under dir. of Zdeněk Kopal): Tables of Supersonic Flow Around Cones of Large Yaw. Tech. Rep. No. 5 (NOrd Contract Nos. 8555 and 9169), Massachusetts Inst. Technol., 1949.
4. Staff of Comput. Section, Center of Anal. (Under dir. of Zdeněk Kopal): Tables of Supersonic Flow Around Cones. Tech. Rep. No. 1 (NOrd Contract No. 9169), Massachusetts Inst. Technol., 1947.
5. Sims, Joseph L.: Tables for Supersonic Flow Around Right Circular Cones at Zero Angle of Attack. NASA SP-3004, 1964.
6. Ames Research Staff: Equations, Tables, and Charts for Compressible Flow. NACA Rep. 1135, 1953. (Supersedes NACA TN 1428.)

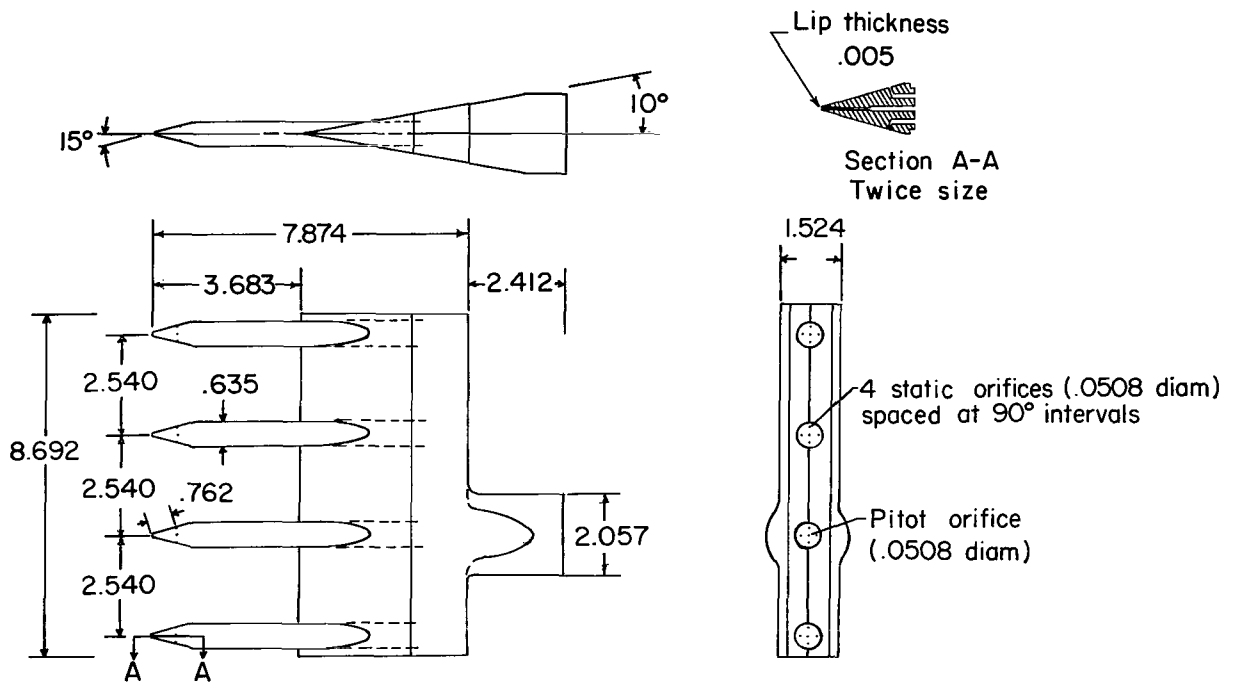


Figure 1.- Calibration rake. All dimensions in centimeters unless otherwise stated.

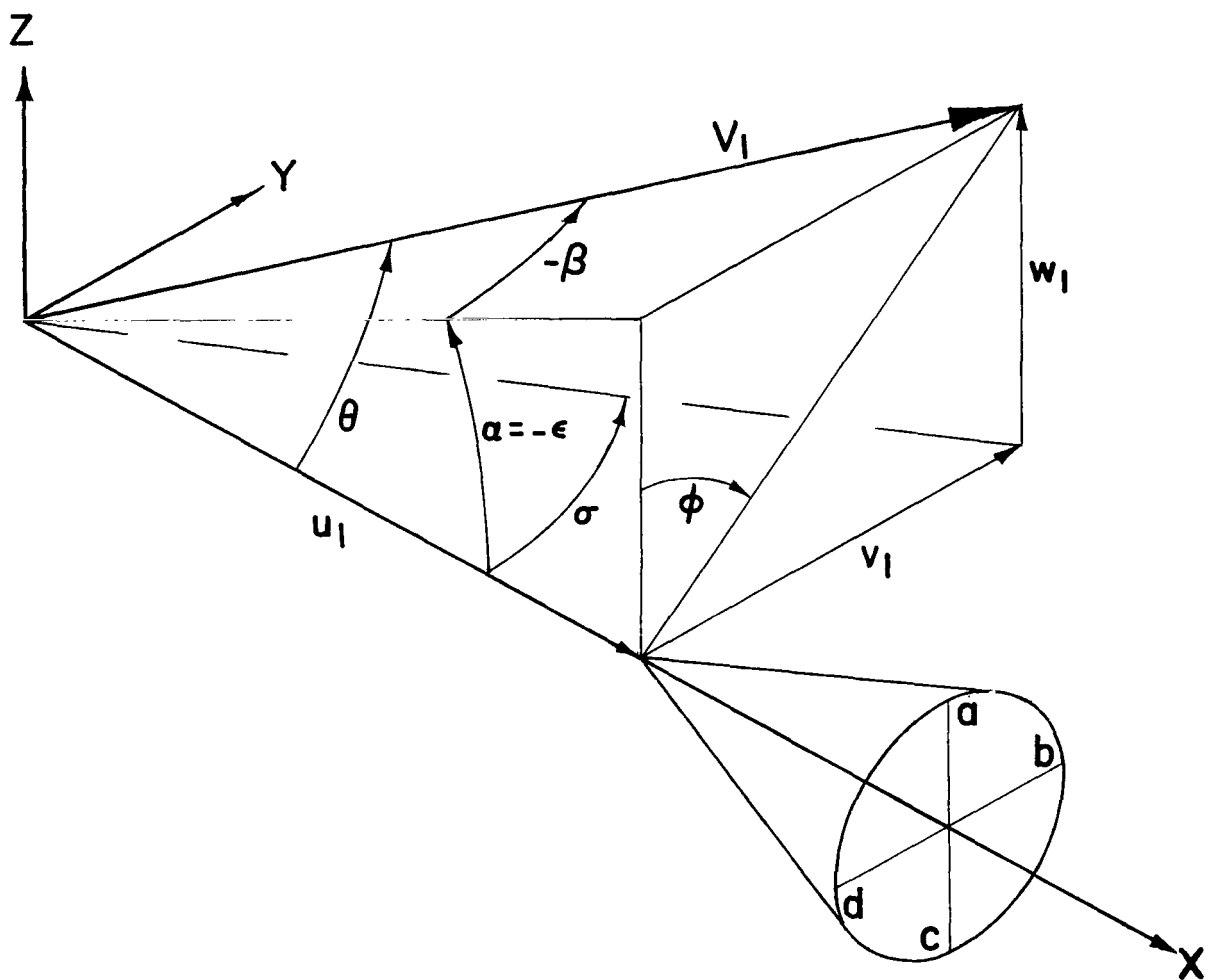
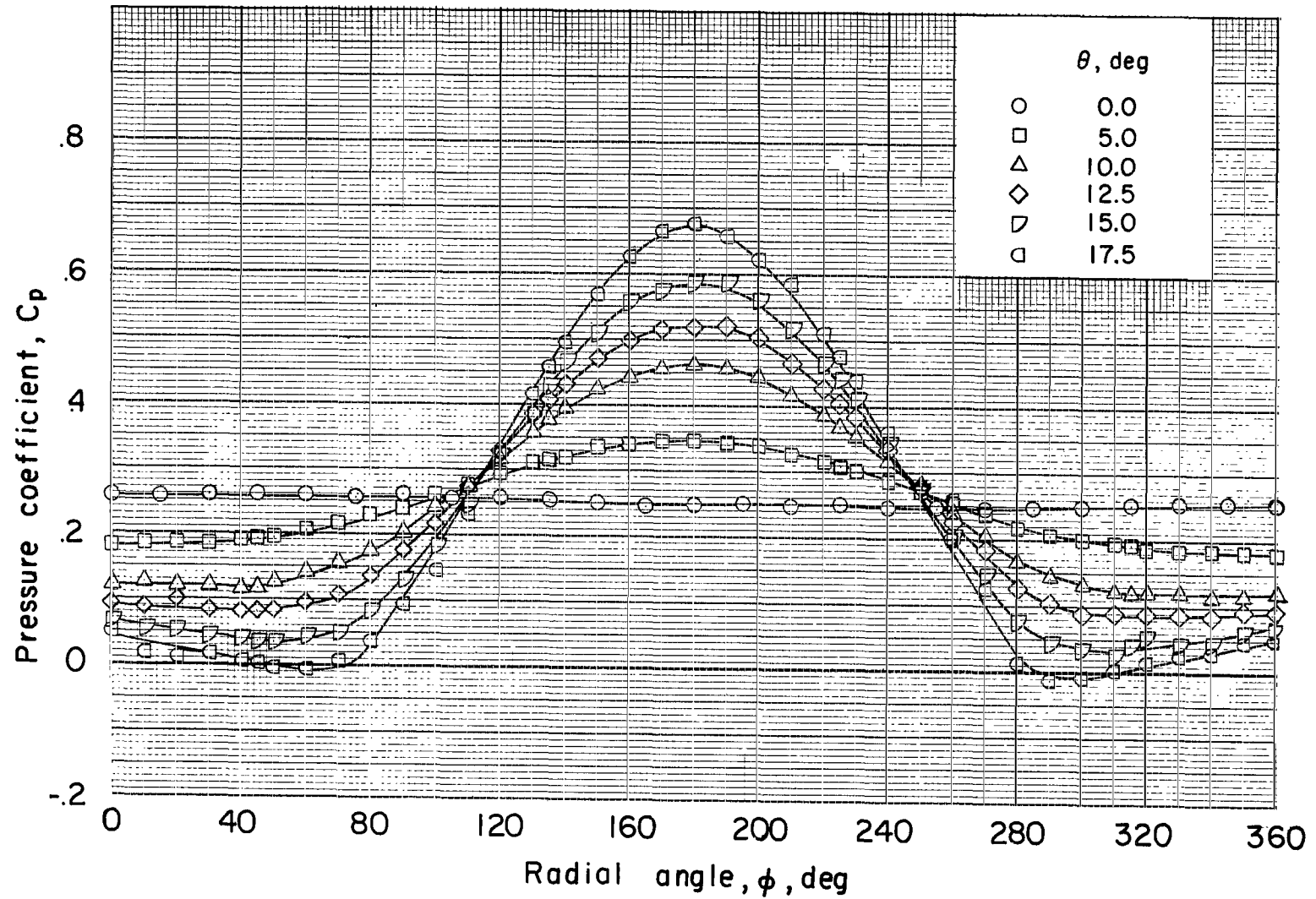
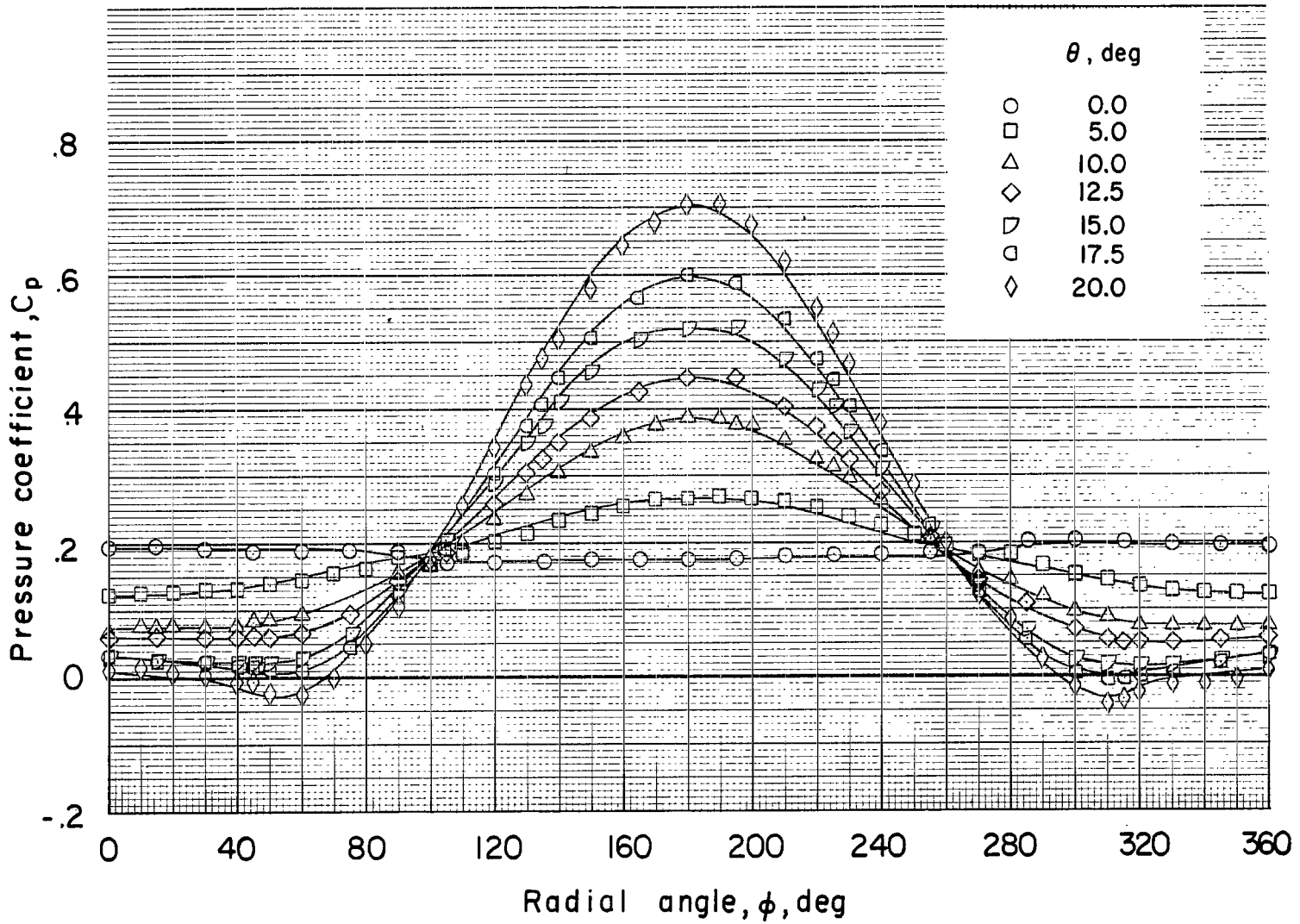


Figure 2.- Orifice designation and angle notation.



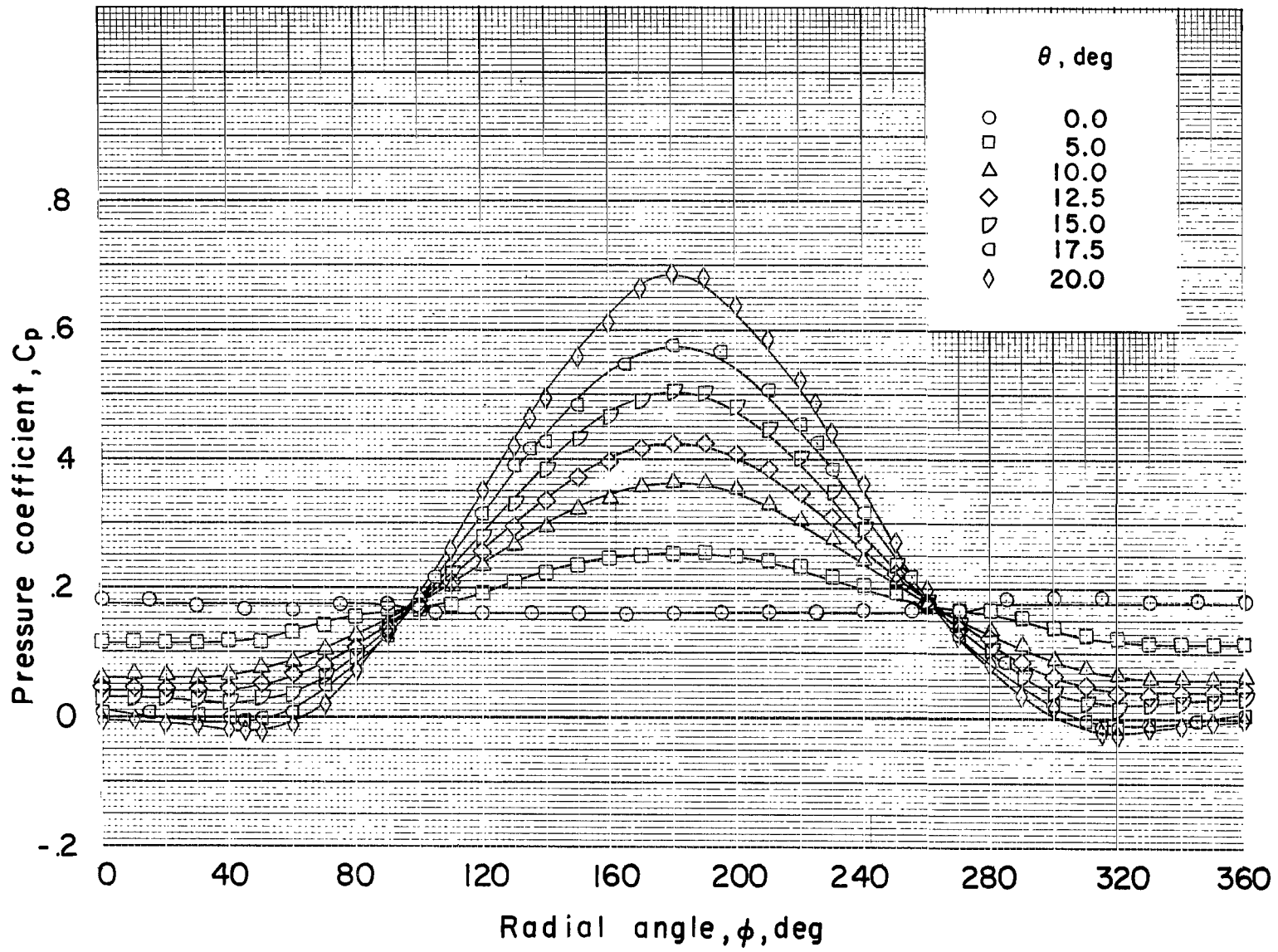
(a) $M_1 = 1.51$.

Figure 3.- Pressure distribution on cone surface.



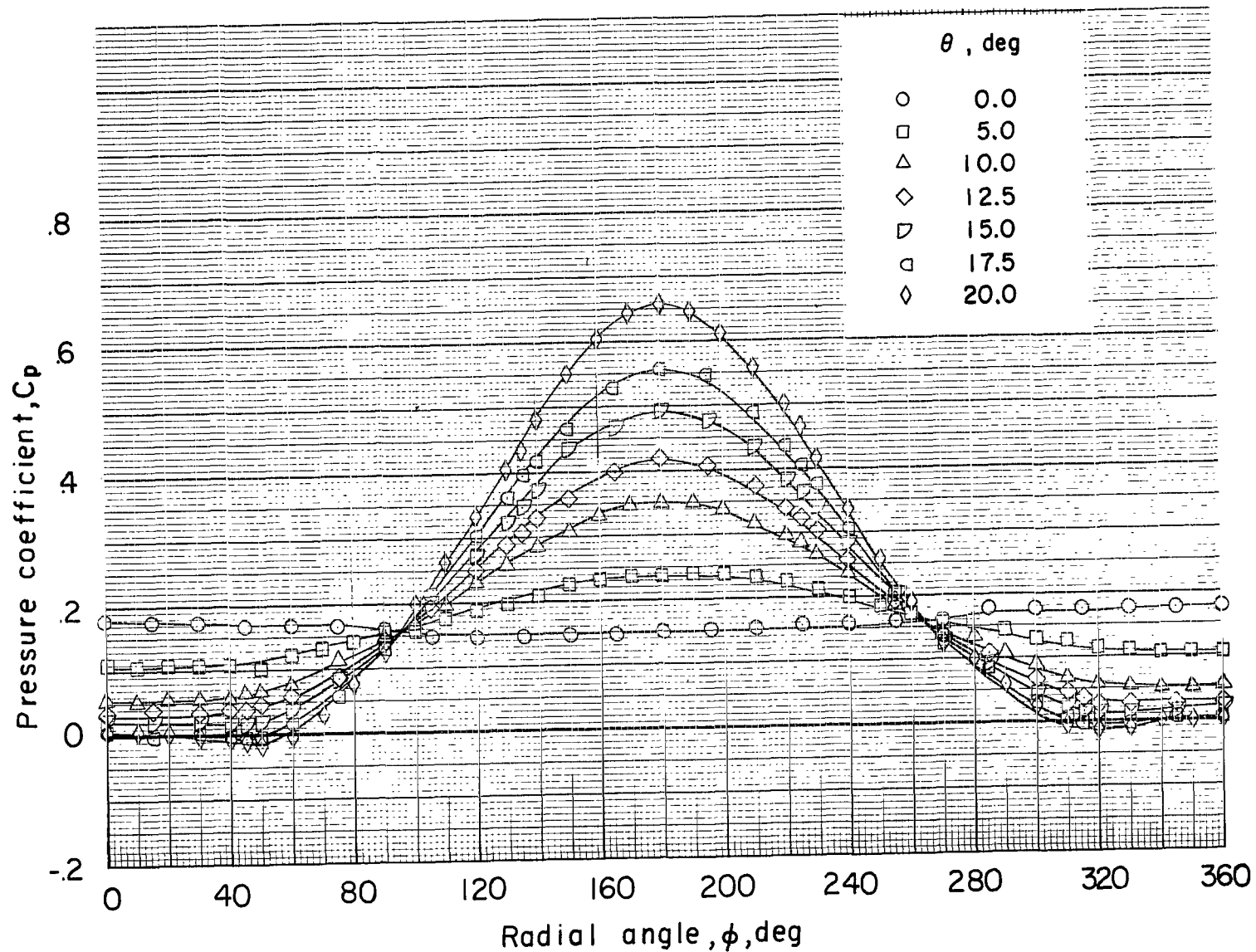
(b) $M_1 = 2.37$.

Figure 3.- Continued.



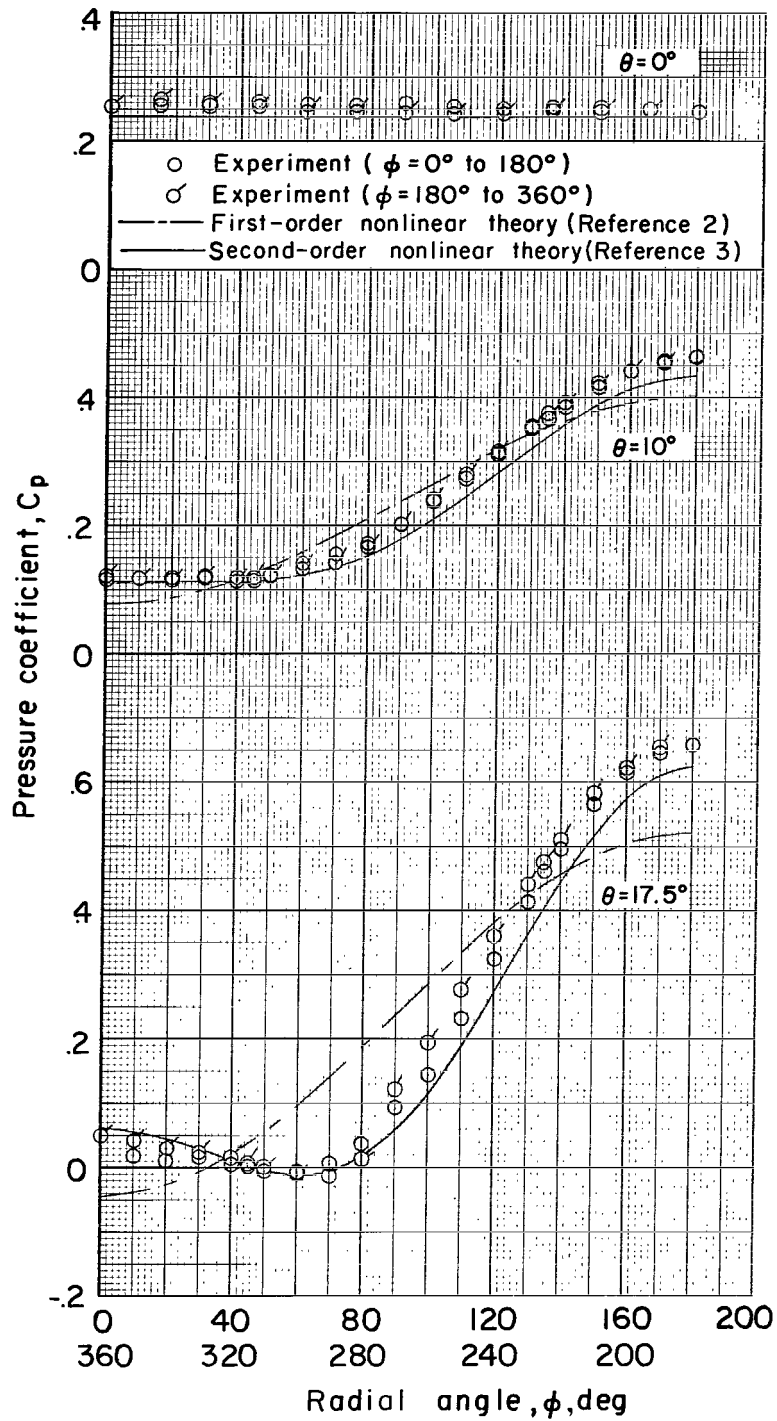
(c) $M_1 = 2.96$.

Figure 3.- Continued.



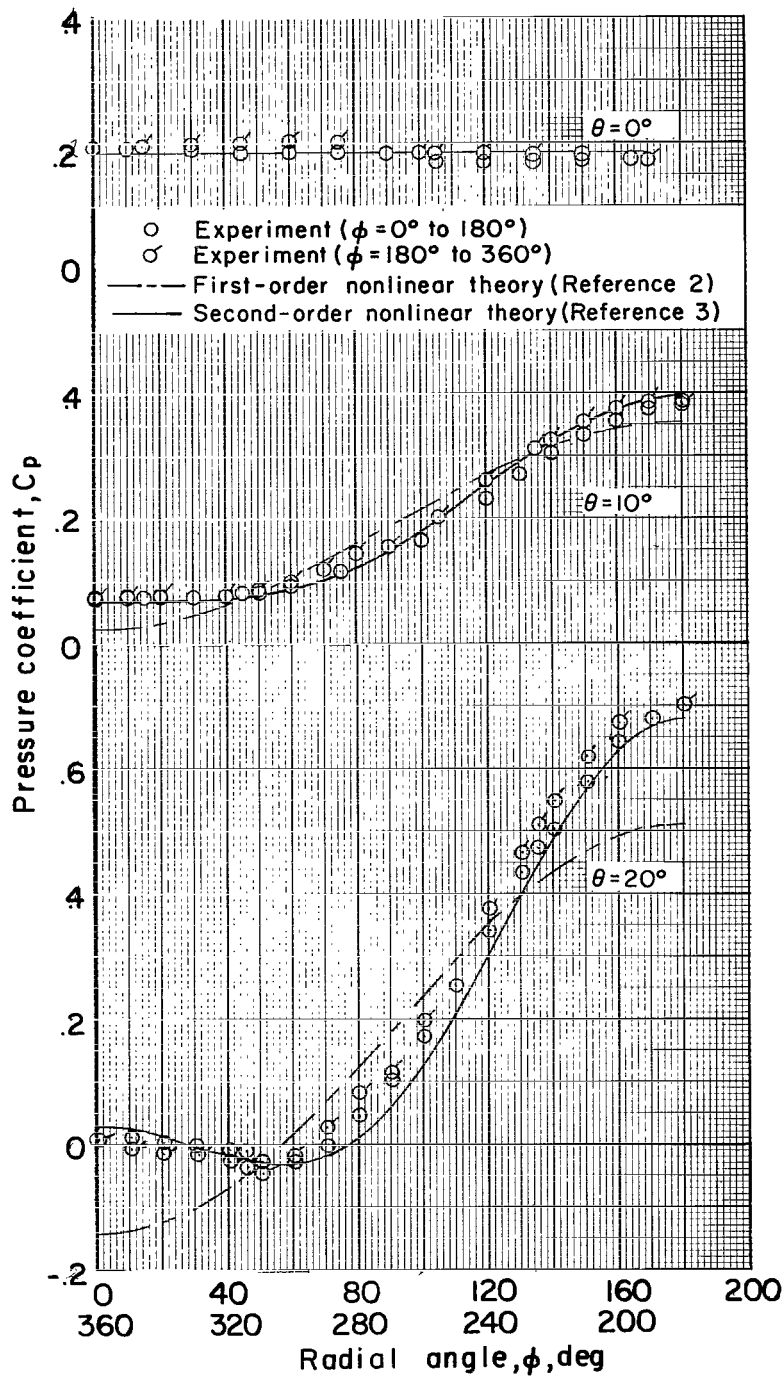
(d) $M_1 = 3.51$.

Figure 3.- Concluded.



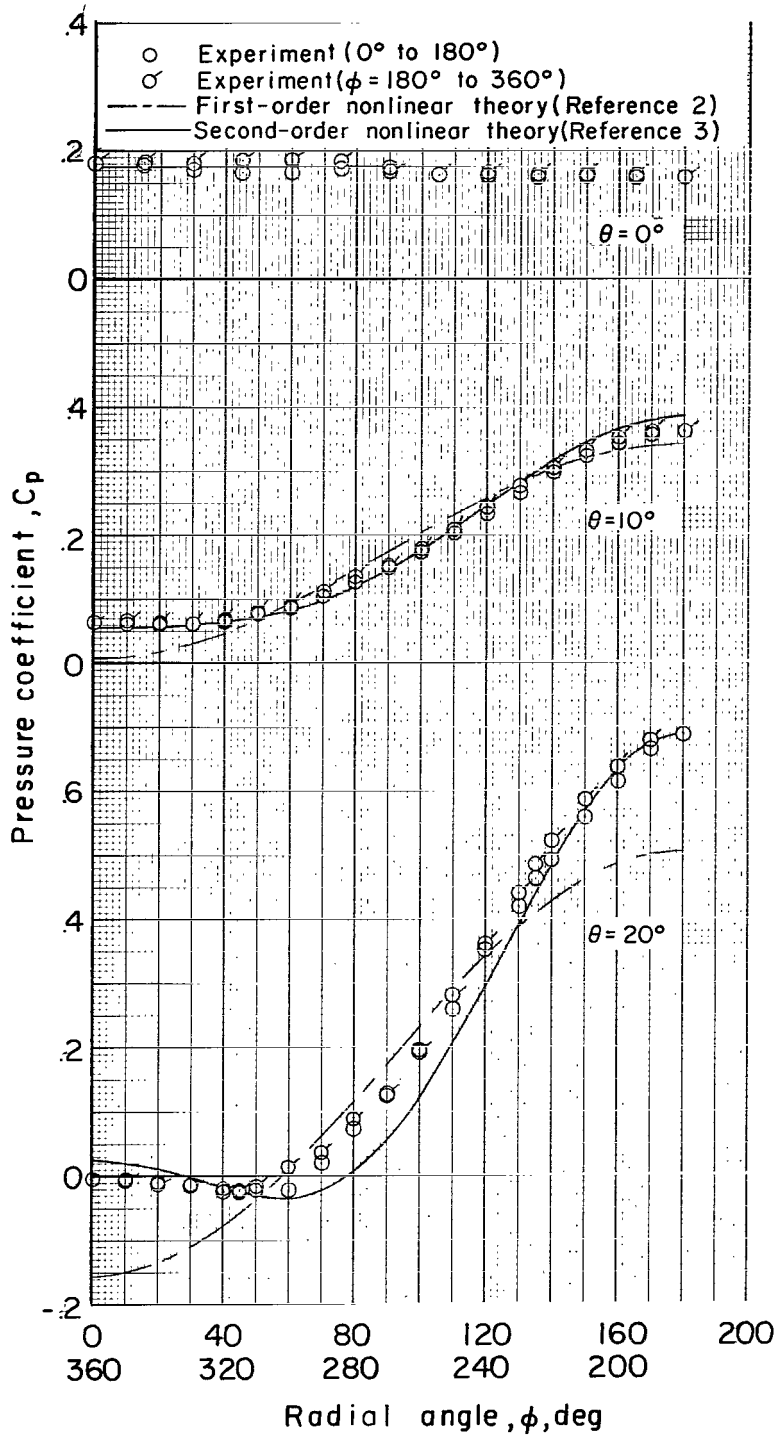
(a) $M_1 = 1.51$.

Figure 4.- Comparison of experimental and theoretical pressure distributions on cone surface.



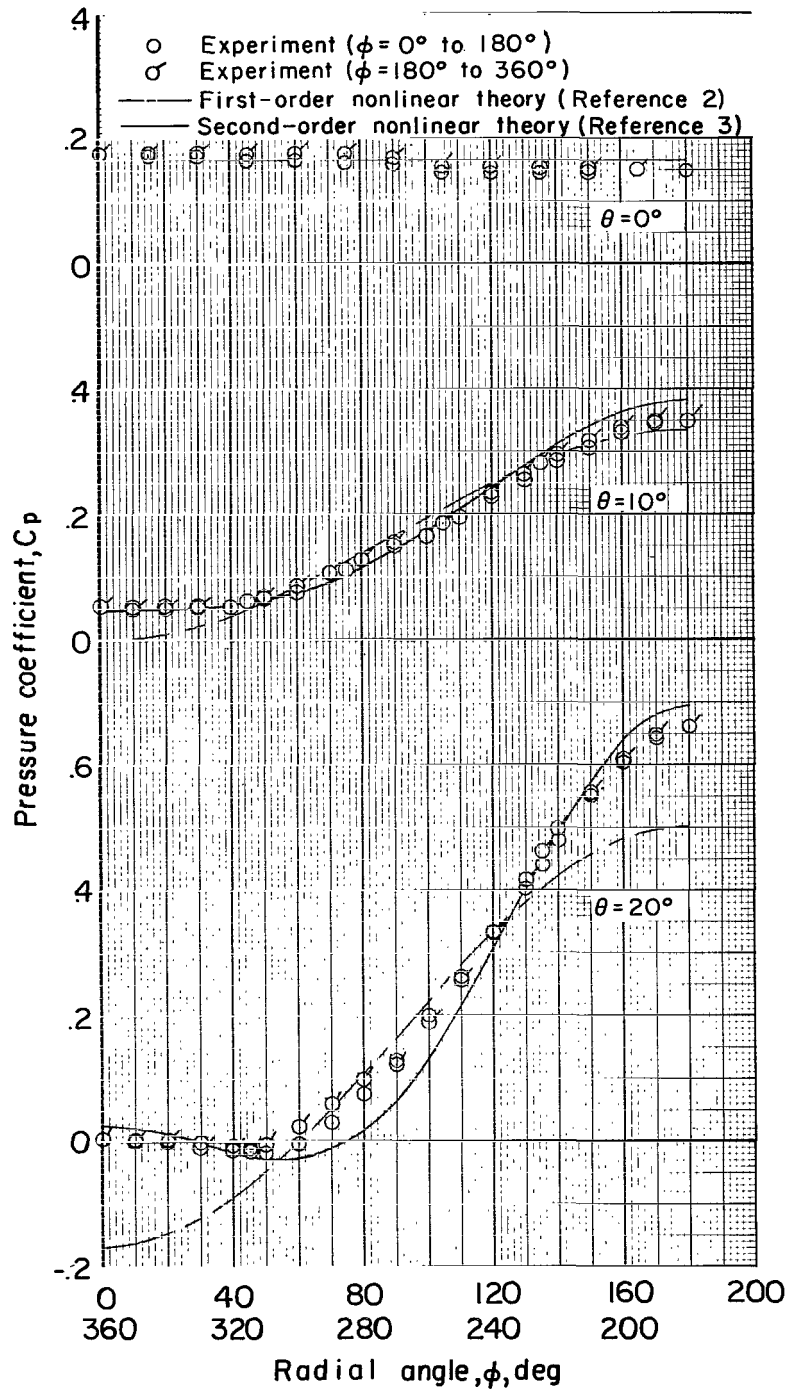
(b) $M_1 = 2.37$.

Figure 4.- Continued.



(c) $M_1 = 2.96$.

Figure 4.- Continued.



(d) $M_1 = 3.51$.

Figure 4.- Concluded.

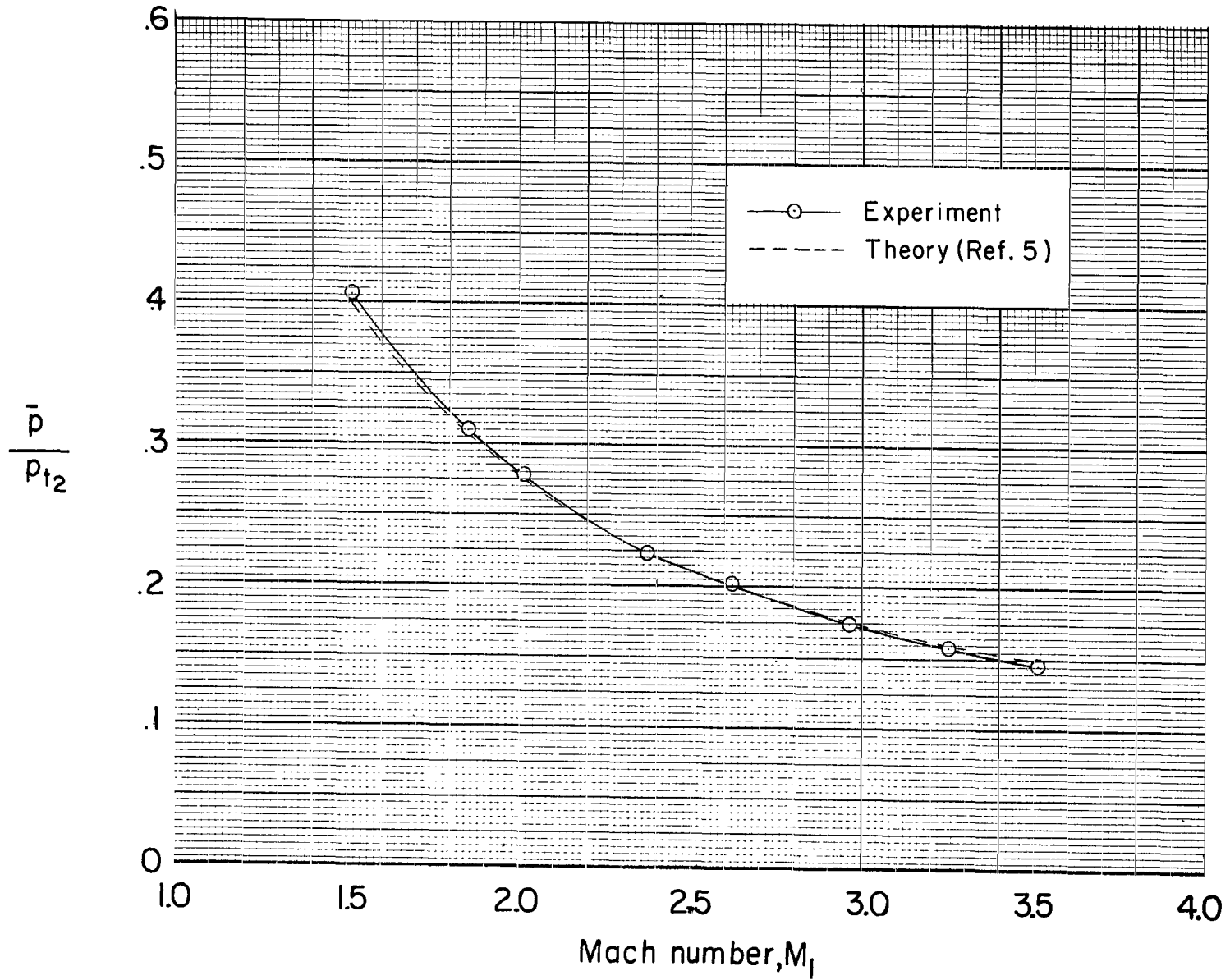
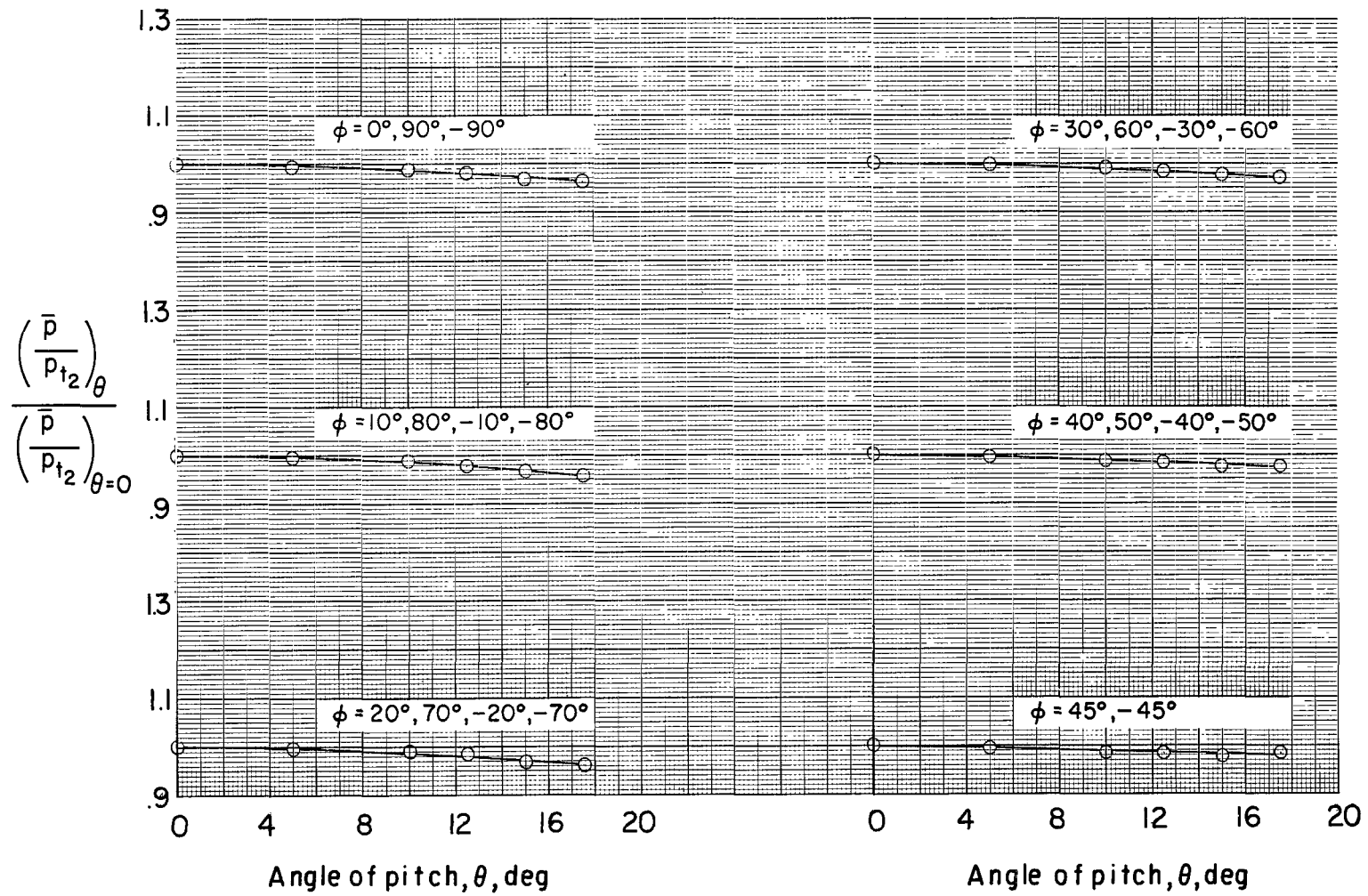
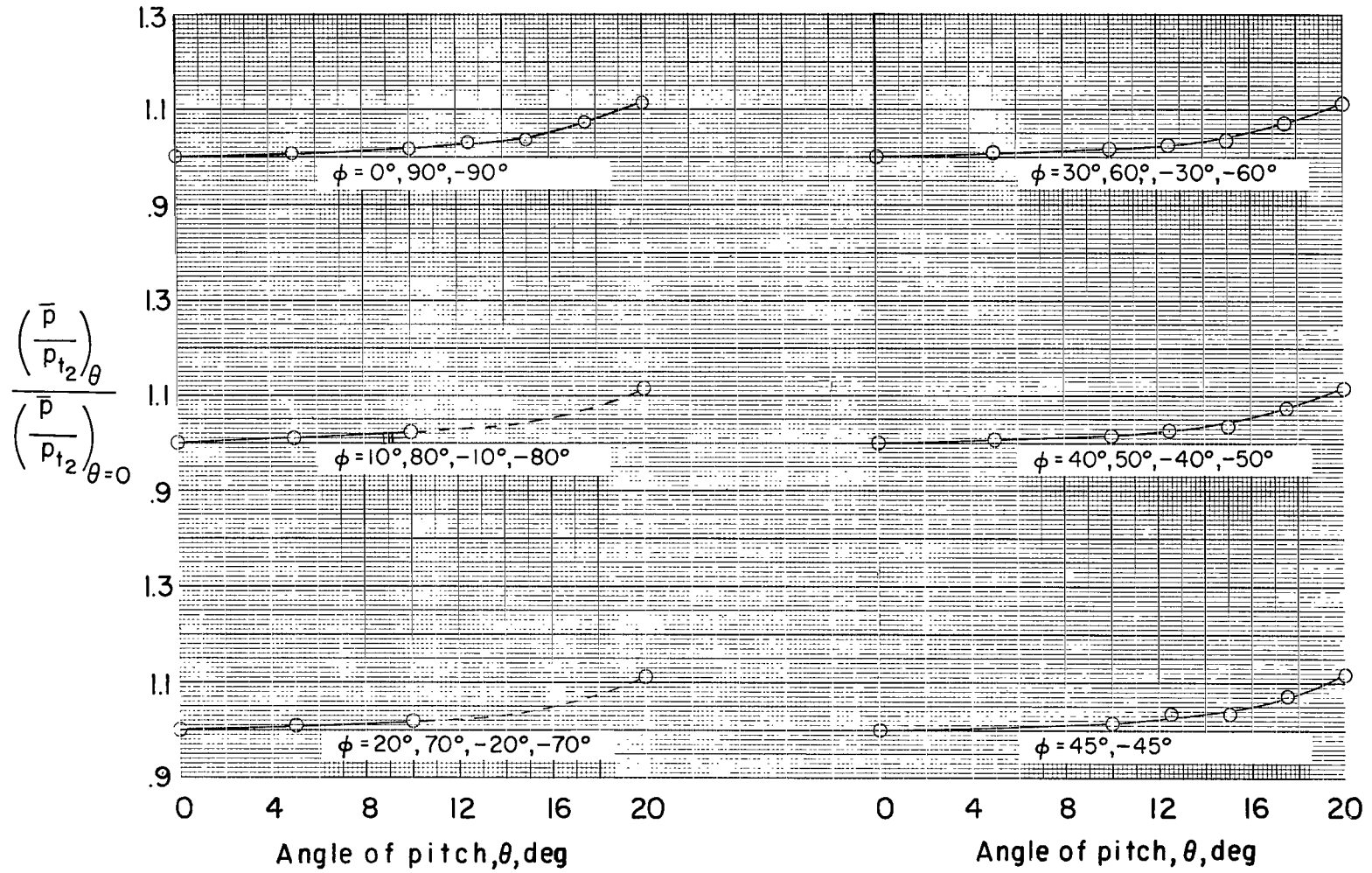


Figure 5.- Effect of Mach number on static-pitot pressure ratio at zero inclination.



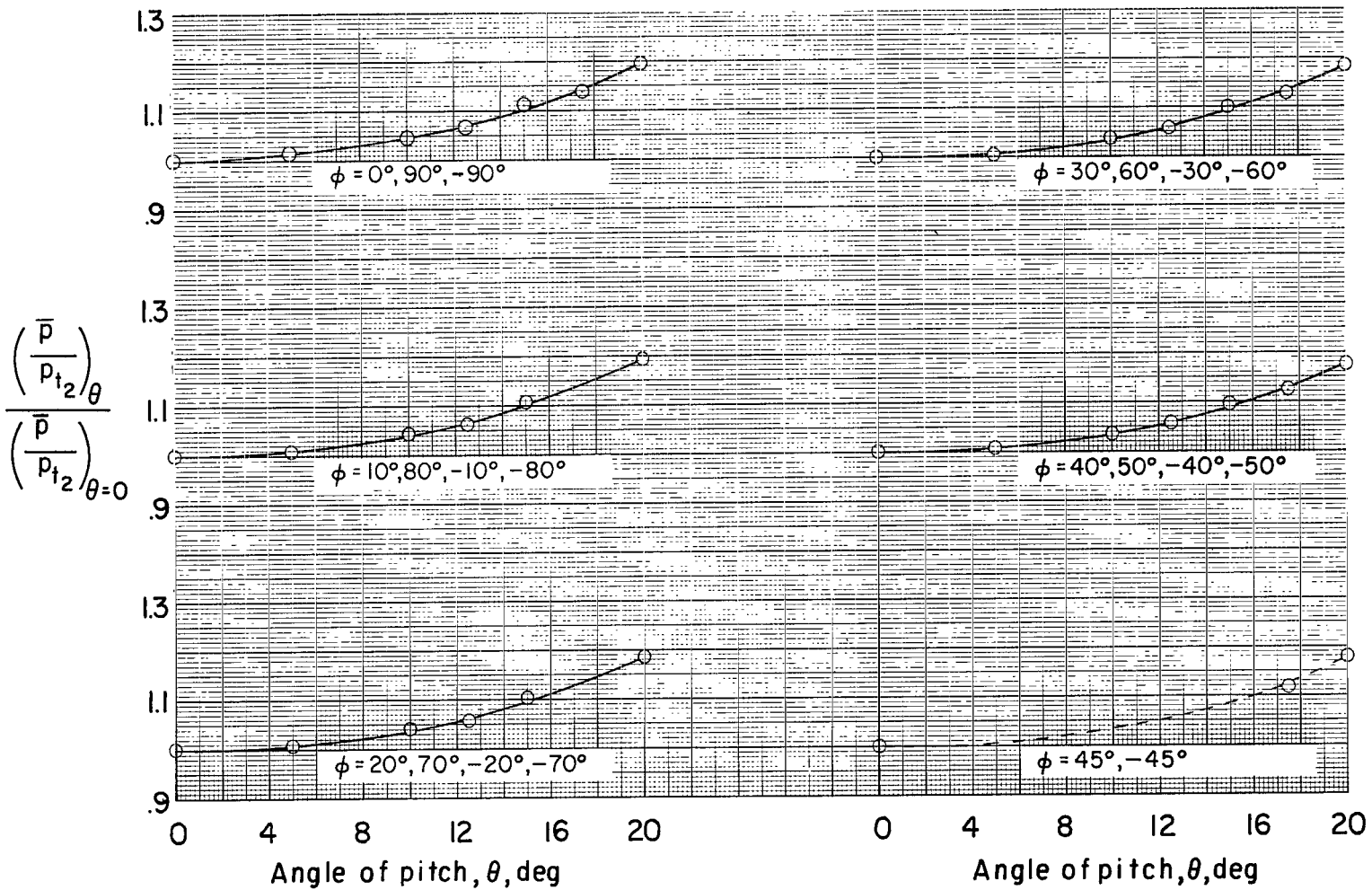
(a) $M_1 = 1.51$.

Figure 6.- Effect of angle of pitch on ratio of average static pressure to pitot pressure. (Dashed portions of curves indicate cross-plotted data.)



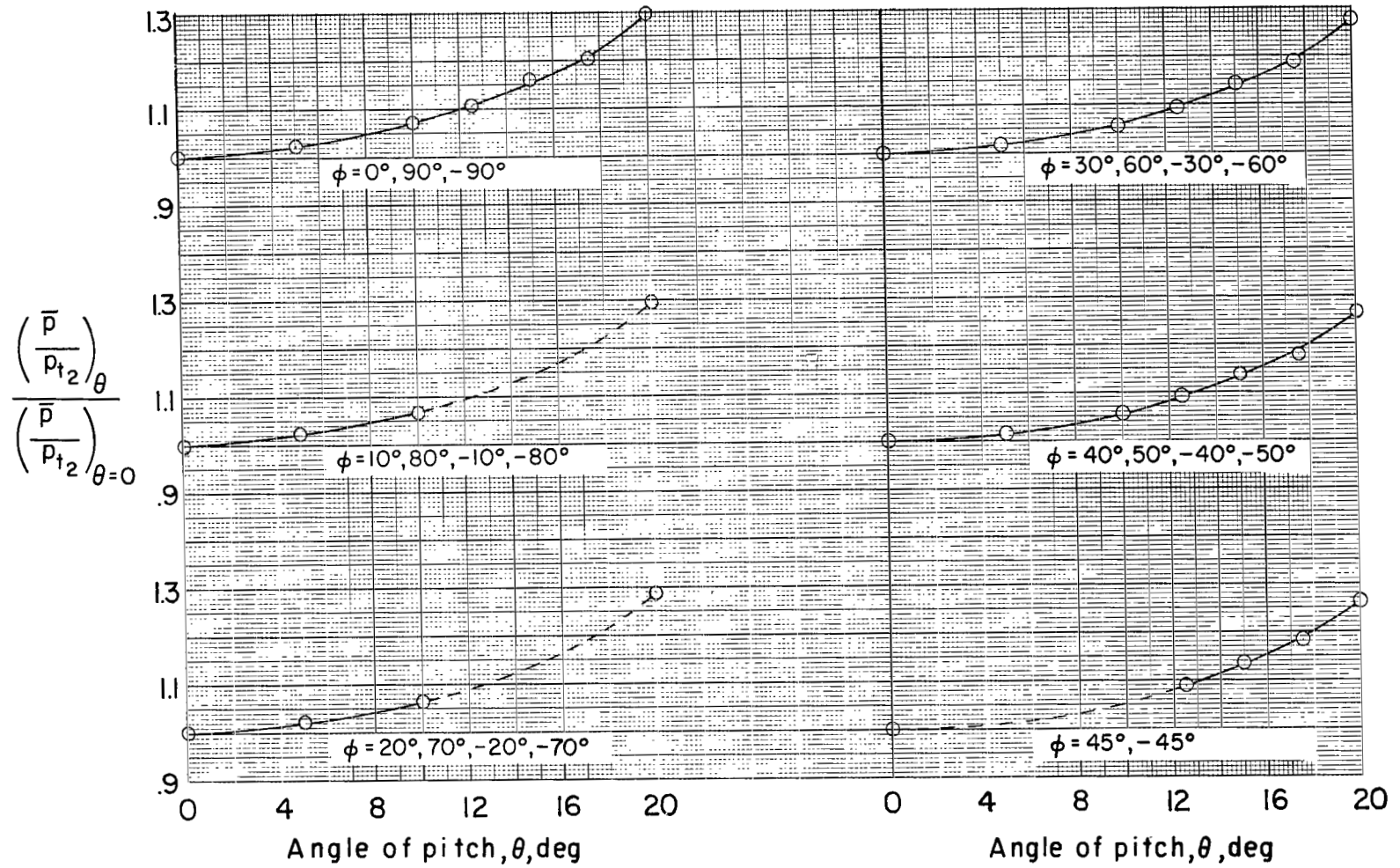
(b) $M_1 = 2.37$.

Figure 6.- Continued.



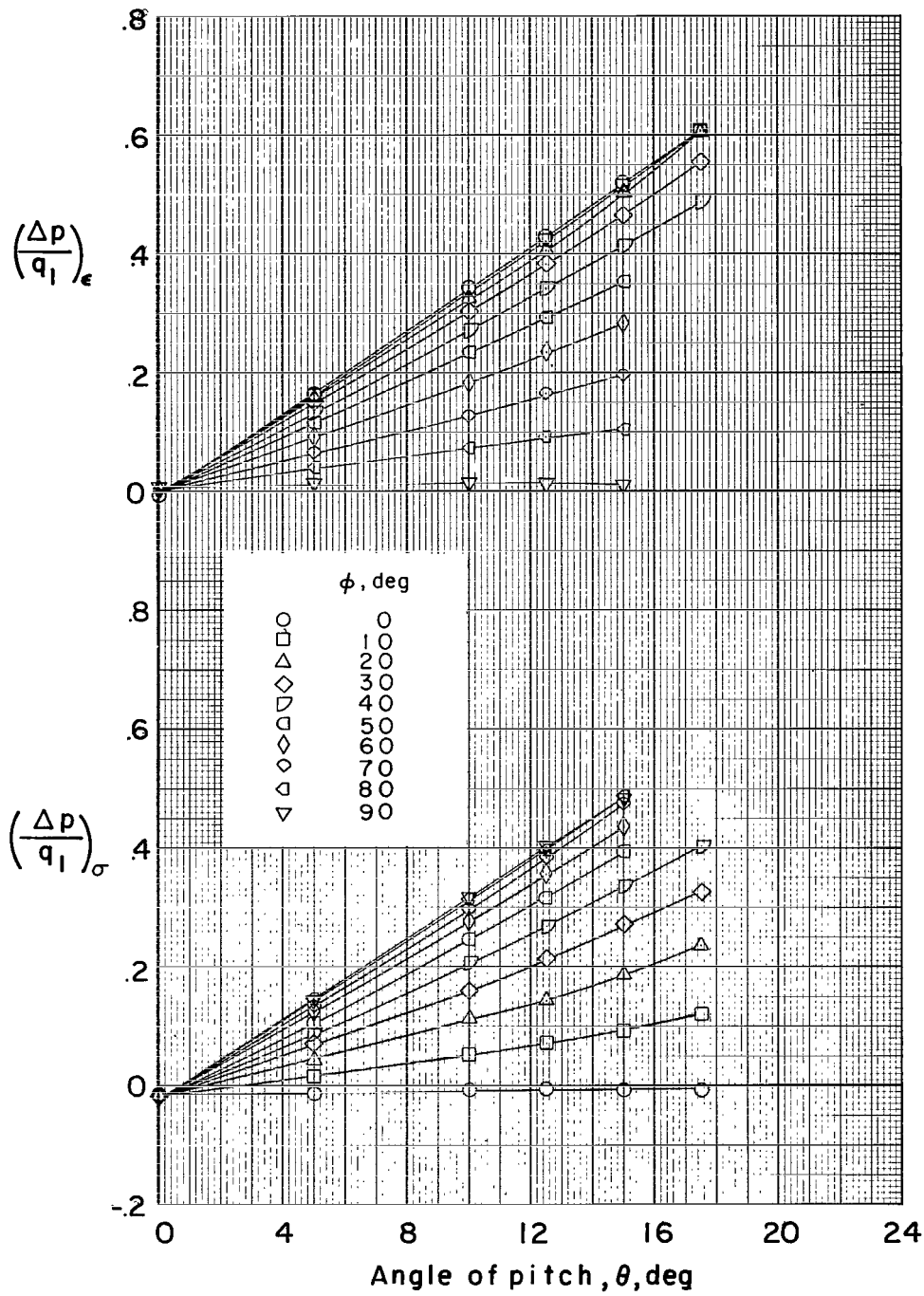
(c) $M_1 = 2.96$.

Figure 6.- Continued.



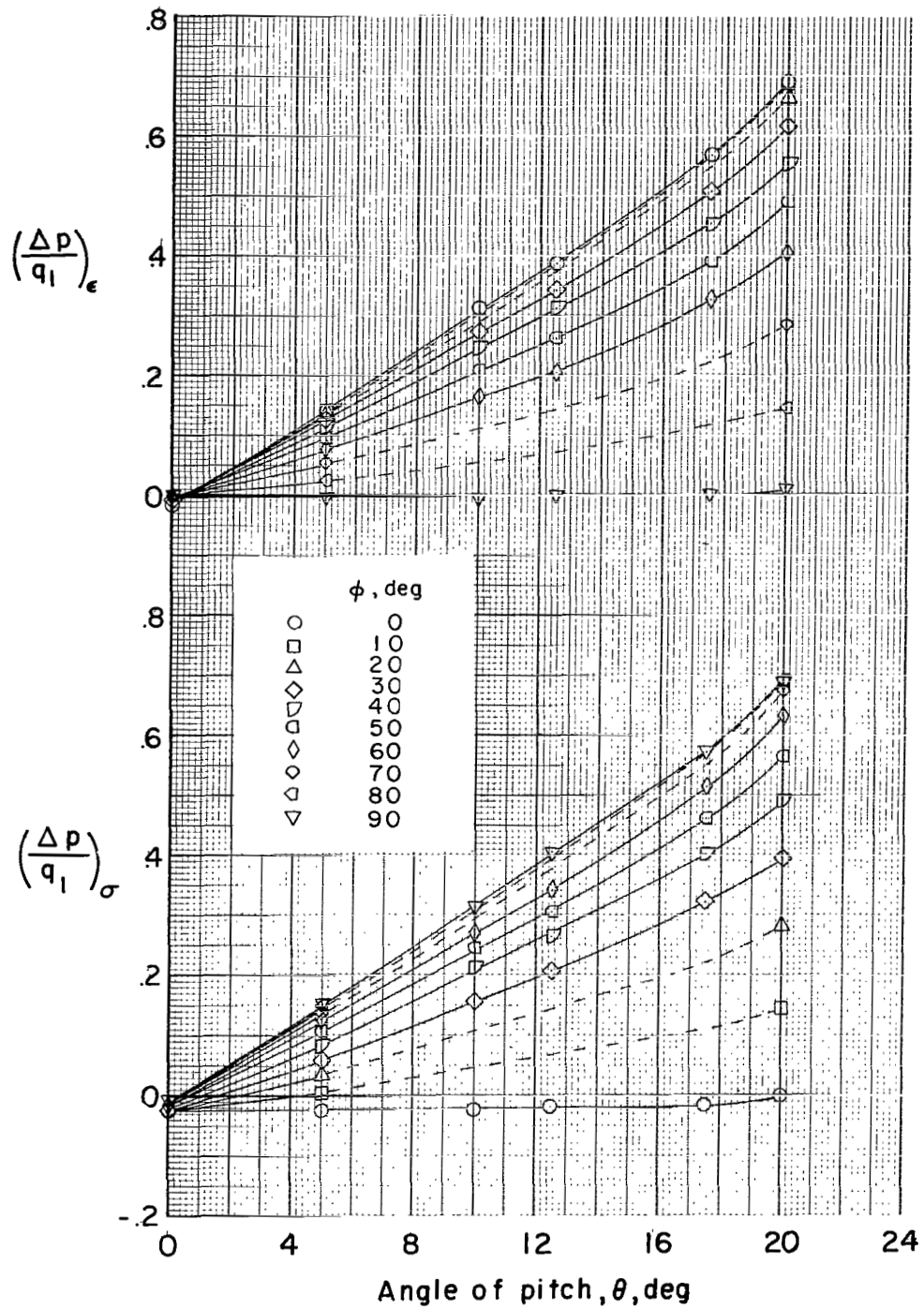
(d) $M_1 = 3.51$.

Figure 6.- Concluded.



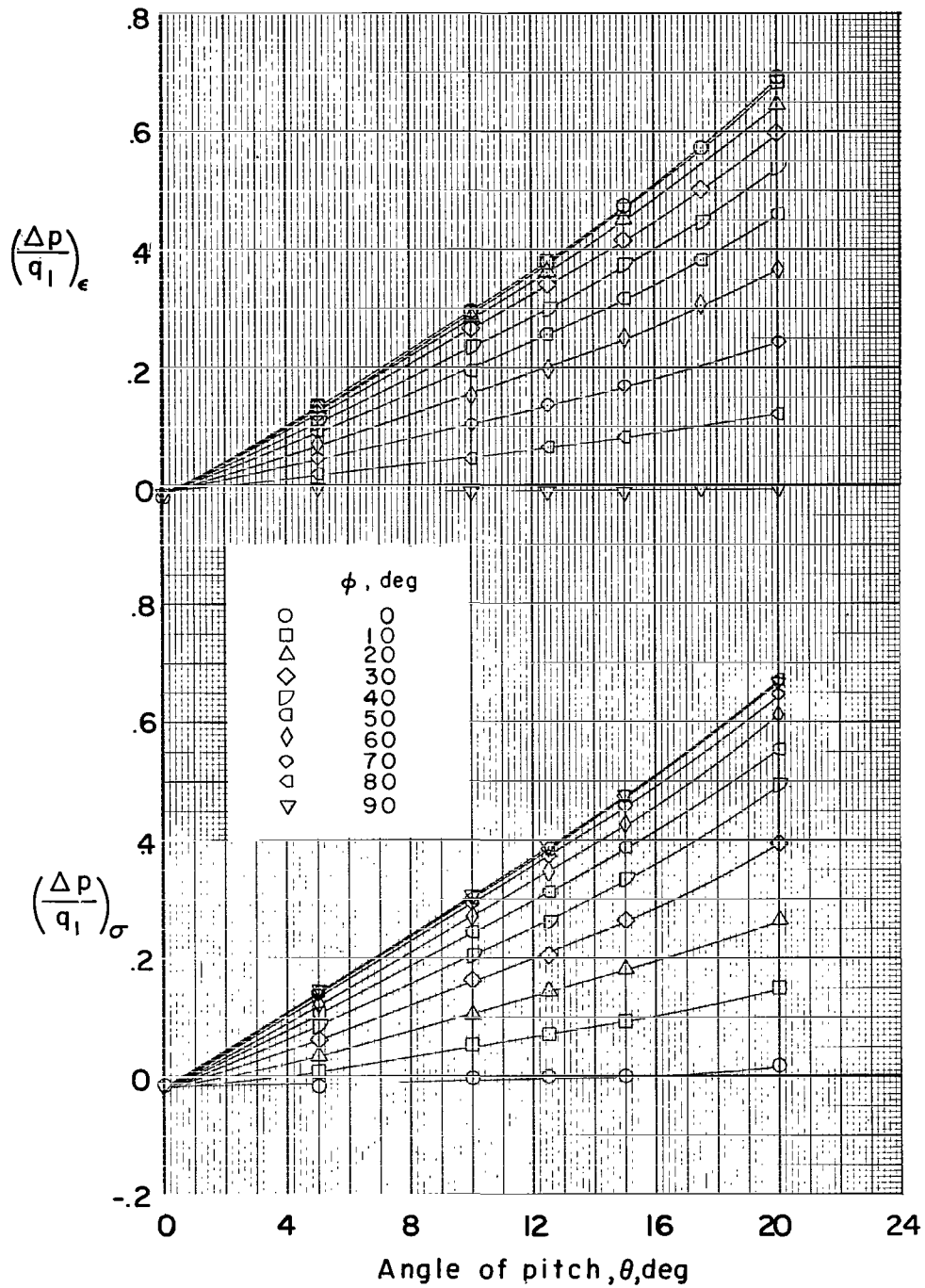
(a) $M_1 = 1.51$.

Figure 7.- Effect of angle of pitch on static-pressure difference coefficient. (Dashed portions of curves indicate cross-plotted data.)



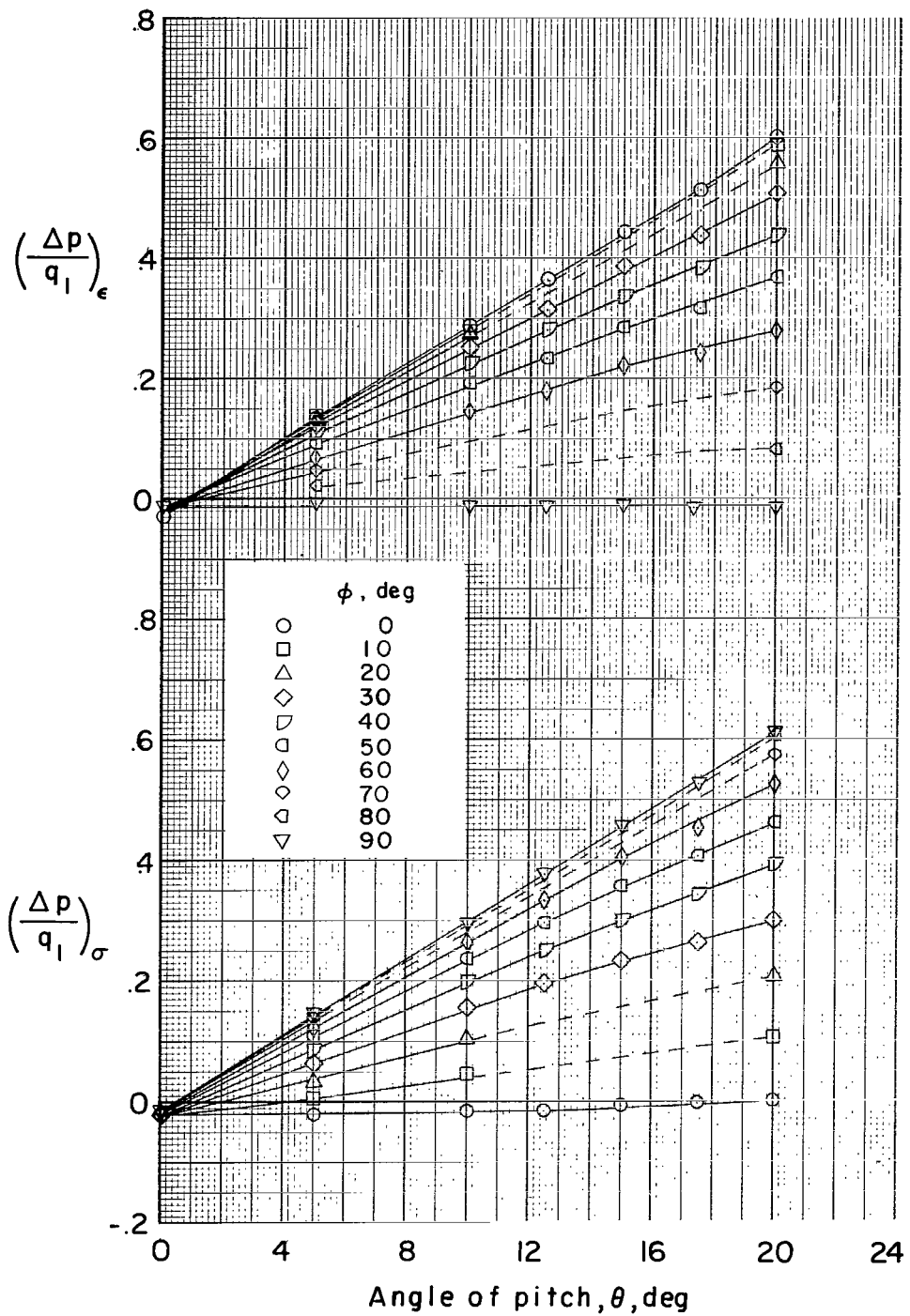
(b) $M_1 = 2.37$.

Figure 7.- Continued.



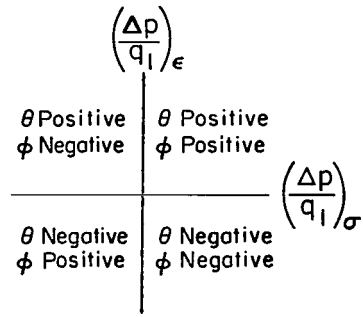
(c) $M_1 = 2.96$.

Figure 7.- Continued.

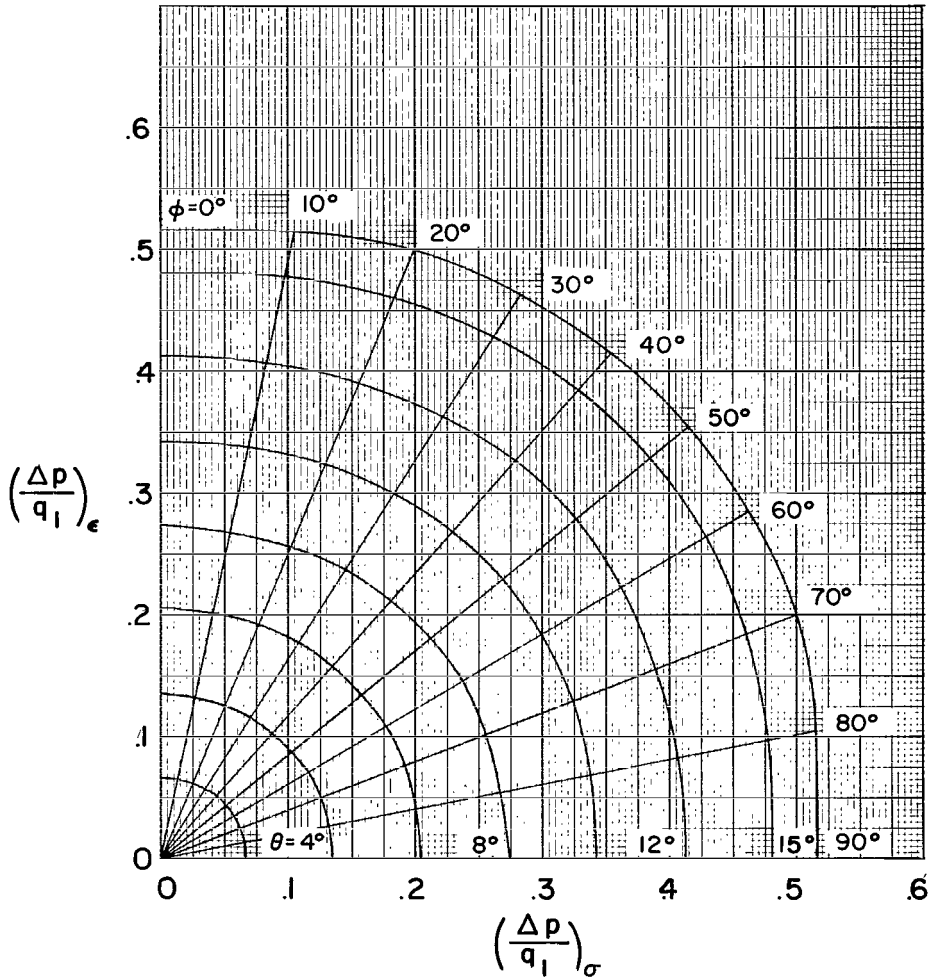


(d) $M_1 = 3.51$.

Figure 7.- Concluded.



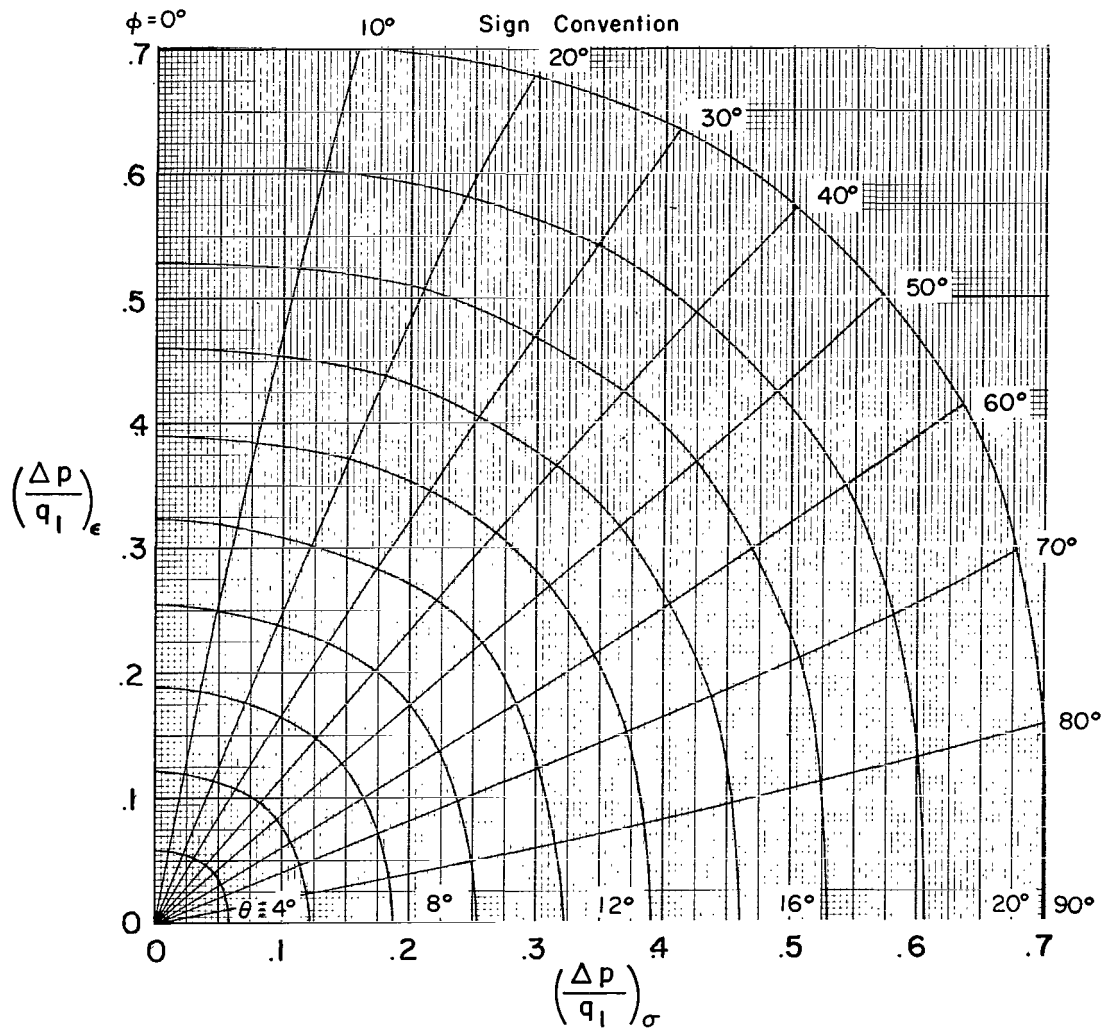
Sign Convention



(a) $M_1 = 1.51$.

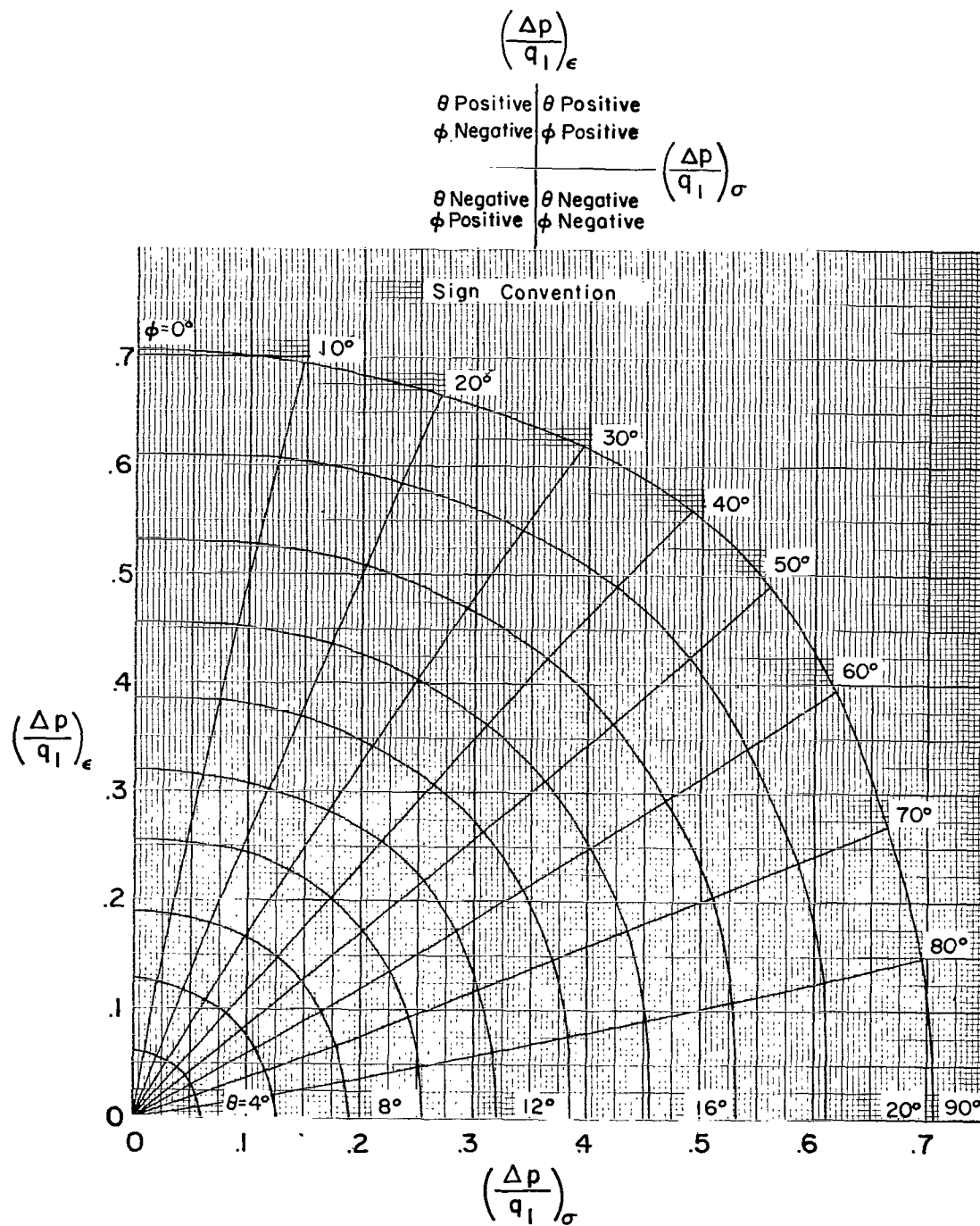
Figure 8.- Chart for determination of pitch and roll angles.

$\left(\frac{\Delta p}{q_1}\right)_\epsilon$	
θ Positive ϕ Negative	θ Positive ϕ Positive
$\left(\frac{\Delta p}{q_1}\right)_\sigma$	
θ Negative ϕ Positive	θ Negative ϕ Negative



(b) $M_1 = 2.37$.

Figure 8.- Continued.

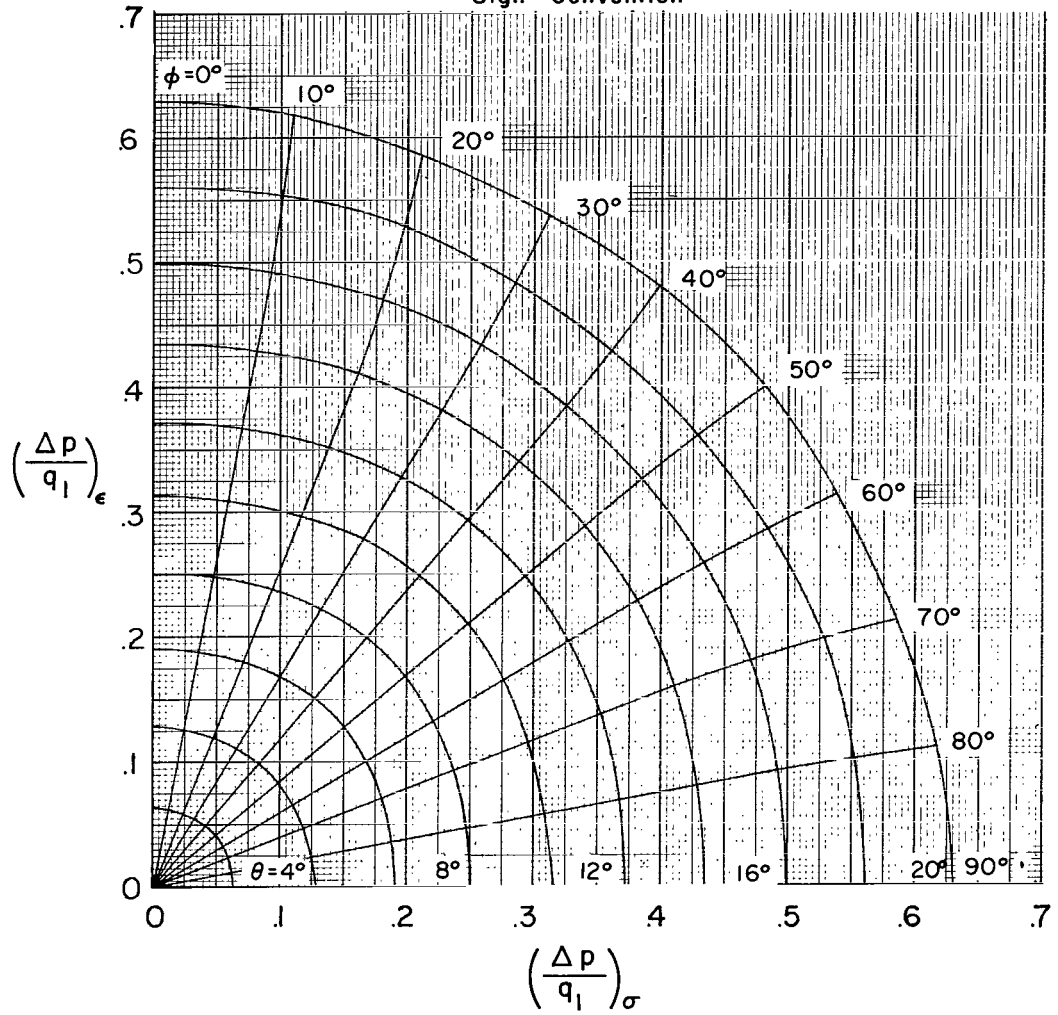


(c) $M_1 = 2.96$.

Figure 8.- Continued.

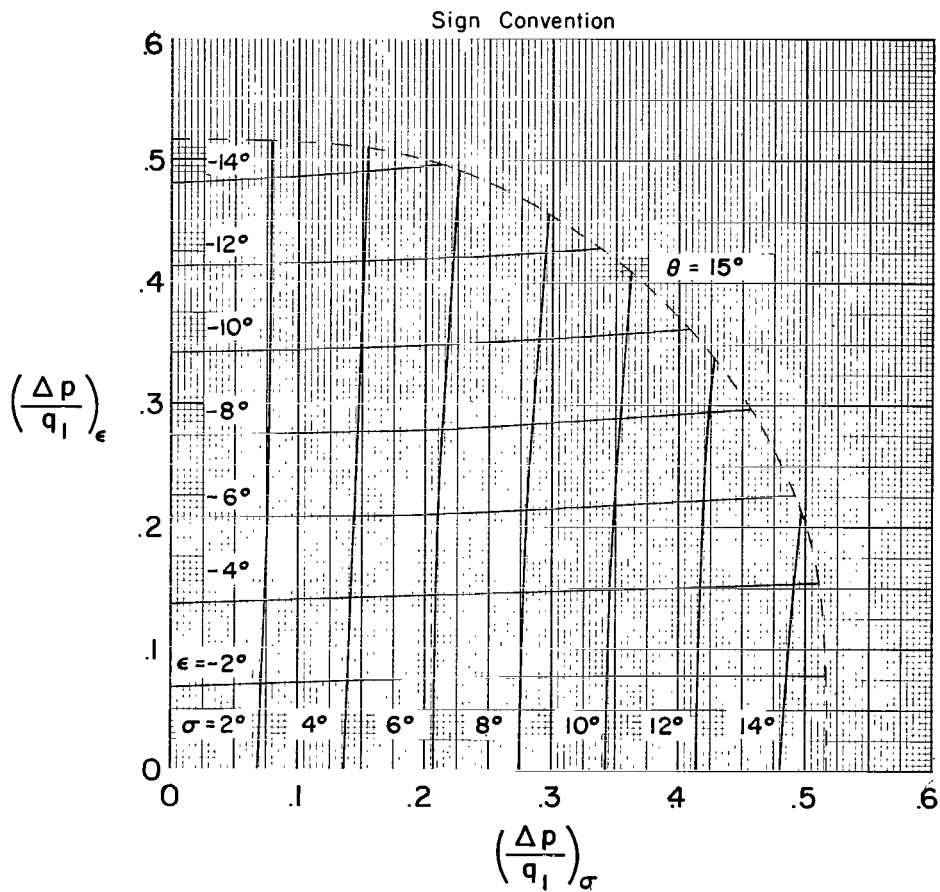
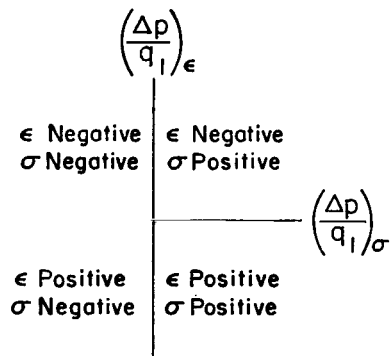
$\left(\frac{\Delta p}{q_1}\right)_\epsilon$		$\left(\frac{\Delta p}{q_1}\right)_\sigma$
θ Positive ϕ Negative	θ Positive ϕ Positive	
<hr style="width: 100%;"/>		
θ Negative ϕ Positive	θ Negative ϕ Negative	

Sign Convention



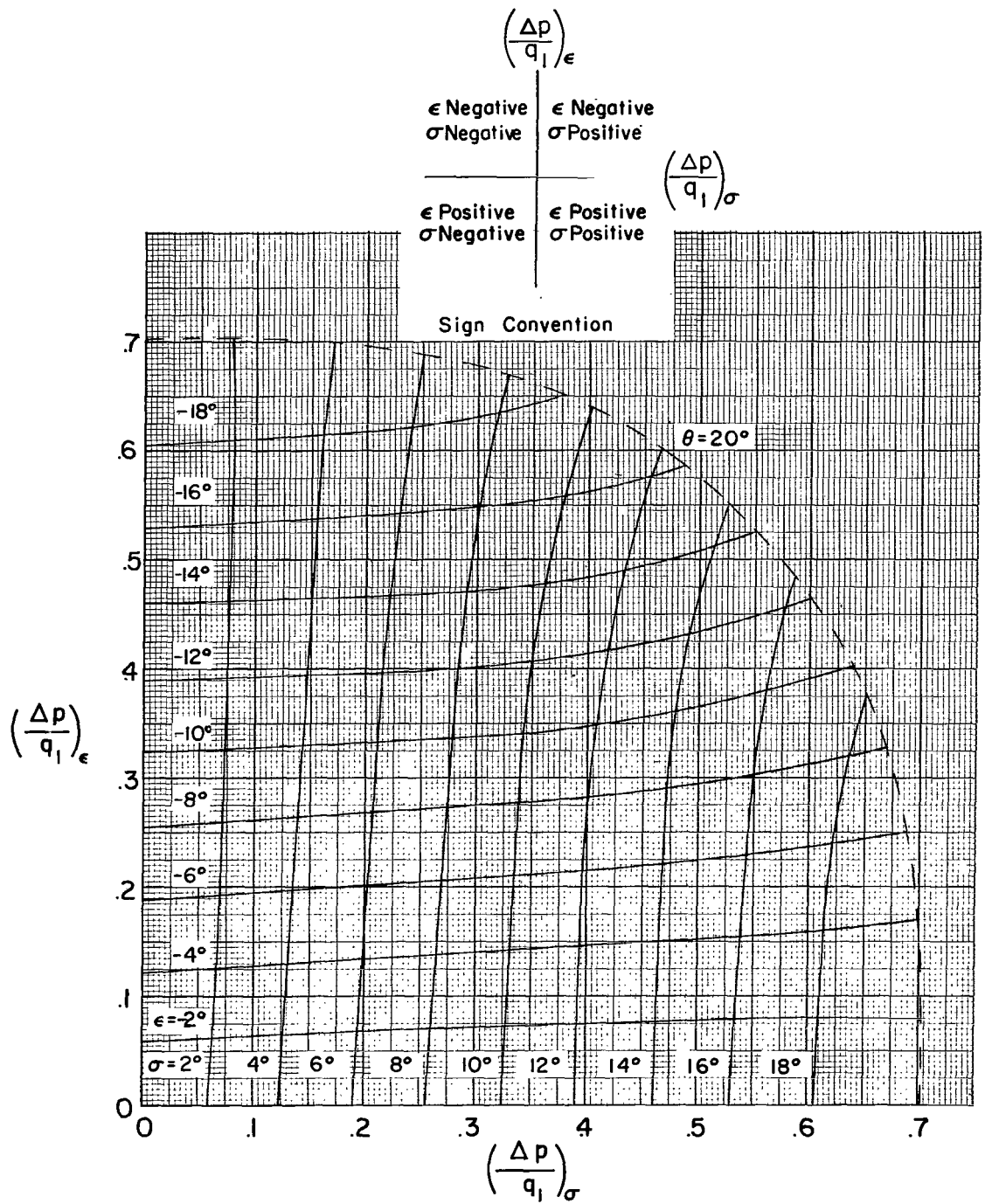
(d) $M_1 = 3.51$.

Figure 8.- Concluded.



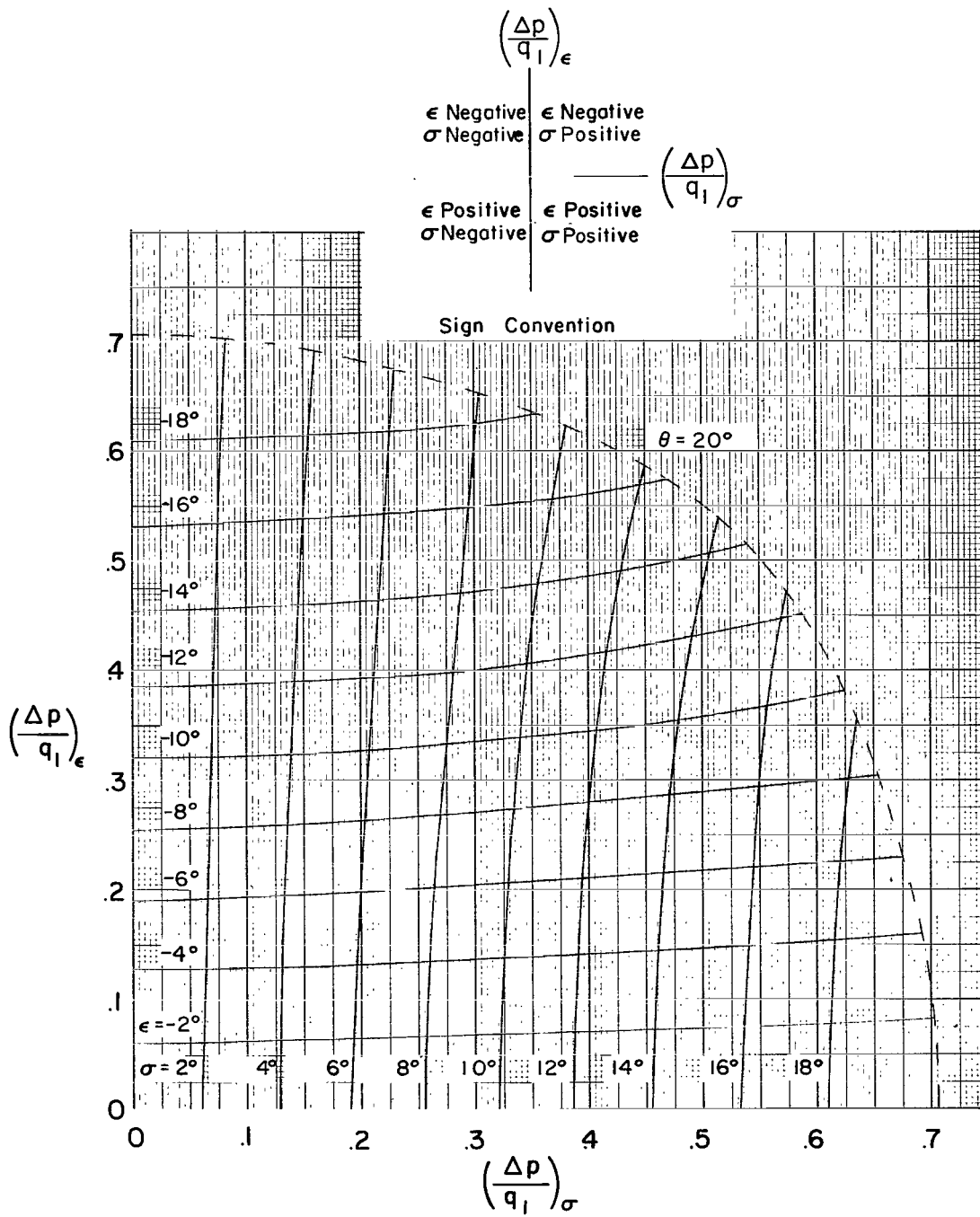
(a) $M_1 = 1.51$.

Figure 9.- Chart for determination of downwash and sidewash angles.



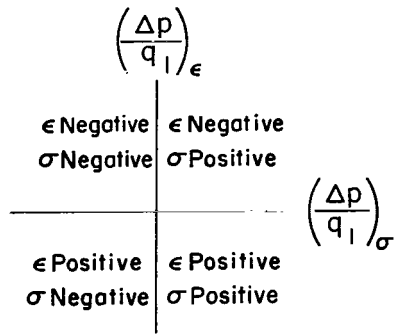
(b) $M_1 = 2.37$.

Figure 9.- Continued.

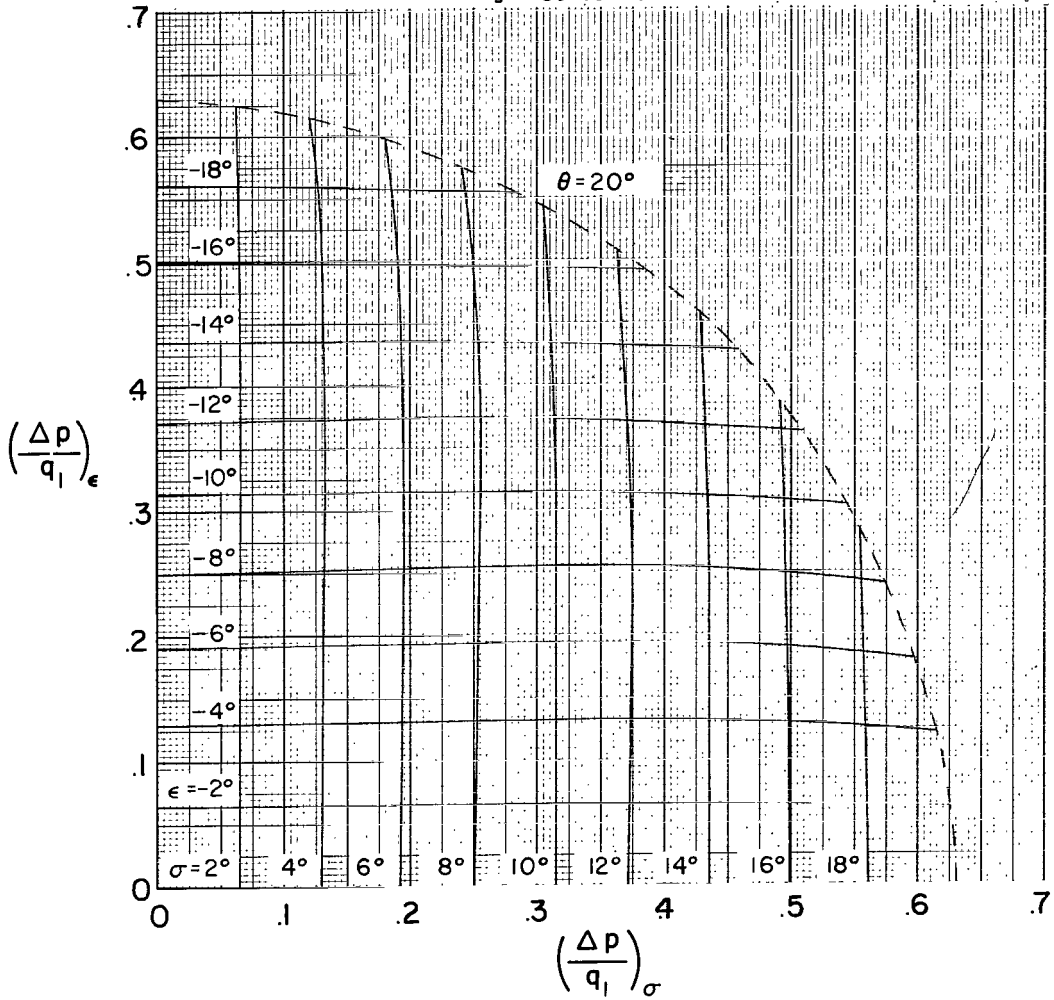


(c) $M_1 = 2.96$.

Figure 9.- Continued.



Sign Convention



(d) $M_1 = 3.51$.

Figure 9.- Concluded.

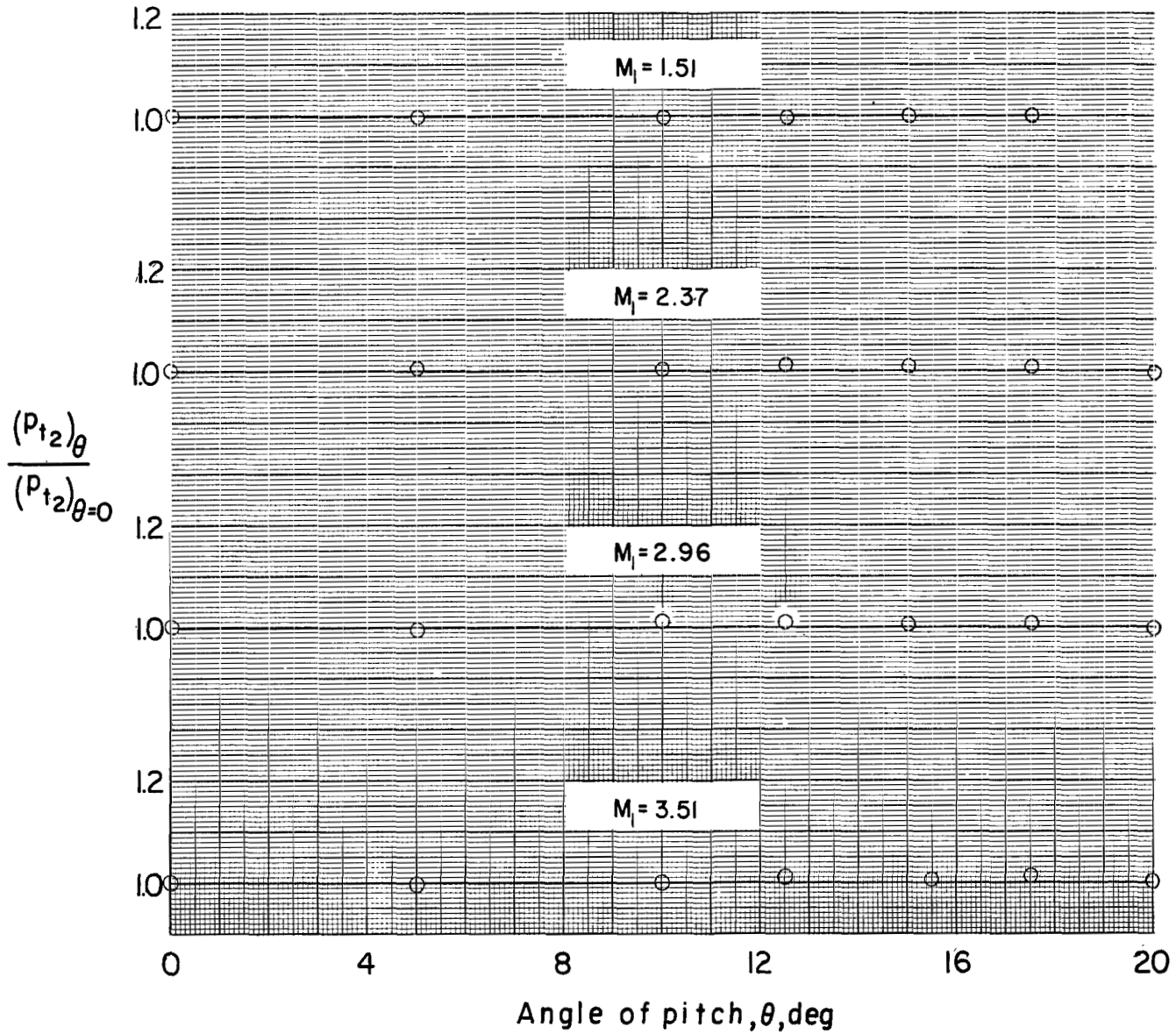


Figure 10.- Effect of inclination on pitot pressure.

FIRST CLASS MAIL

CIL 001 26 51 3DS 68194 00903
AIR FORCE WEAPON LABORATORY/AFWL/
WRIGHT AIR FORCE BASE, NEW MEXICO 87117

DR. J. H. COOPER, JR., CHIEF TECHNICAL
PERSONNEL

POSTMASTER: If Undeliverable (Section 158
Postal Manual) Do Not Return

"The aeronautical and space activities of the United States shall be conducted so as to contribute . . . to the expansion of human knowledge of phenomena in the atmosphere and space. The Administration shall provide for the widest practicable and appropriate dissemination of information concerning its activities and the results thereof."

— NATIONAL AERONAUTICS AND SPACE ACT OF 1958

NASA SCIENTIFIC AND TECHNICAL PUBLICATIONS

TECHNICAL REPORTS: Scientific and technical information considered important, complete, and a lasting contribution to existing knowledge.

TECHNICAL NOTES: Information less broad in scope but nevertheless of importance as a contribution to existing knowledge.

TECHNICAL MEMORANDUMS: Information receiving limited distribution because of preliminary data, security classification, or other reasons.

CONTRACTOR REPORTS: Scientific and technical information generated under a NASA contract or grant and considered an important contribution to existing knowledge.

TECHNICAL TRANSLATIONS: Information published in a foreign language considered to merit NASA distribution in English.

SPECIAL PUBLICATIONS: Information derived from or of value to NASA activities. Publications include conference proceedings, monographs, data compilations, handbooks, sourcebooks, and special bibliographies.

TECHNOLOGY UTILIZATION PUBLICATIONS: Information on technology used by NASA that may be of particular interest in commercial and other non-aerospace applications. Publications include Tech Briefs, Technology Utilization Reports and Notes, and Technology Surveys.

Details on the availability of these publications may be obtained from:

SCIENTIFIC AND TECHNICAL INFORMATION DIVISION
NATIONAL AERONAUTICS AND SPACE ADMINISTRATION
Washington, D.C. 20546